JOC The Journal of Organic Chemistry

ARTICLE

pubs.acs.org/joc

Synthesis of a Series of Aromatic Benziporphyrins and Heteroanalogues via Tripyrrane-Like Intermediates Derived from Resorcinol and 2-Methylresorcinol†

Timothy D. Lash,* Kae Miyake, Linlin Xu, and Gregory M. Ferrence

Department of Chemistry, Illinois State University, Normal, Illinois 61790-4160, United States

Supporting Information

ABSTRACT: Tripyrrane analogues were prepared by reacting resorcinol or 2-methylresorcinol with 2 equiv of an acetoxymethylpyrrole in the presence of *p*-toluenesulfonic acid and calcium chloride. Following removal of the benzyl ester protective groups, the resorcinol-derived benzitripyrrane was reacted with a pyrrole dialdehyde to give an aromatic hydroxyoxybenziporphyrin. However, furan and thiophene dialdehydes gave highly insoluble products that could not be fully characterized. The methylresorcinol-derived tripyrrane analogue reacted with pyrrole, furan, thiophene, and selenophene dialdehydes to give unstable porphyrinoids that were further oxidized with [bis(trifluoroacetoxy)iodo]benzene to give stable benziporphyrin derivatives. These oxidized benziporphyrins showed strongly diatropic properties by proton NMR spectroscopy where the differences in chemical shifts ($\Delta\delta$) were >18 ppm in some cases. The selenophene-derived system was further characterized by X-ray crystallography, and these results showed that one of the pyrrole subunits in this crowded structure was tilted by 21° relative to the mean macrocyclic plane. The tripyrrolic system reacted with silver(I) acetate to give the corresponding silver(III) organometallic complex. Regioselective alkylation with methyl or ethyl iodide and potassium carbonate gave diastereomeric mixtures of *N*-alkyl derivatives, and the *N*-ethyl substitution products showed highly diastereotopic characteristics.

INTRODUCTION

Benziporphyrins are porphyrin analogues with a benzene ring in place of one of the usual pyrrolic subunits.[1−4] These systems have been widely studied and show a diversity of spectroscopic and chemical properties.[1−9] Although simple benziporphyrins like **1** and **2** are nonaromatic,[1−3,5,6] substituted benziporphyrins vary considerably and may be moderately[10−12] or strongly diatropic.[2,3,13−17]

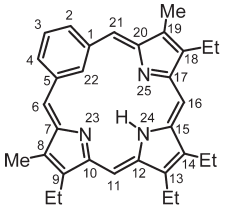

1 (Benziporphyrin)

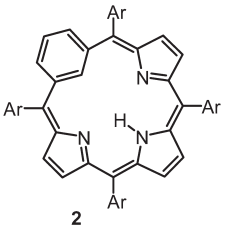

2

Dimethoxybenziporphyrins **3a** and **4a** show significant diatropic character because of the electron-donating properties of the methoxy substituents which introduce dipolar canonical forms like **3′** and **4′** that possess porphyrin-like 18π electron delocalization pathways.[10−12] The internal CH (22-H) gives rise to relatively upfield resonances at 5.07 and 5.84 ppm for **3a** and **4a**, respectively. This effect is much reduced for 3-methylbenziporphyrins **3b** and **4b** because the alkyl substituent prevents the methoxy unit from taking on the correct geometry to allow optimal interactions between the oxygen lone pair electrons and the π-system.[10−12]

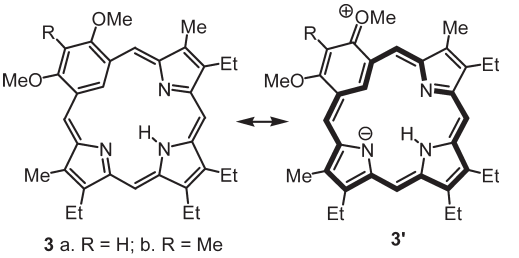

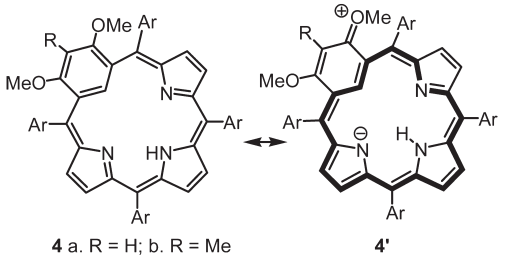

However, addition of TFA affords the related dications which show dramatically increased diatropicity. For instance, $\mathbf{3a}H_2^{2+}$

Received: May 27, 2011
Published: June 21, 2011

   dx.doi.org/10.1021/jo201098c | *J. Org. Chem.* 2011, 76, 6295–6308

Scheme 1

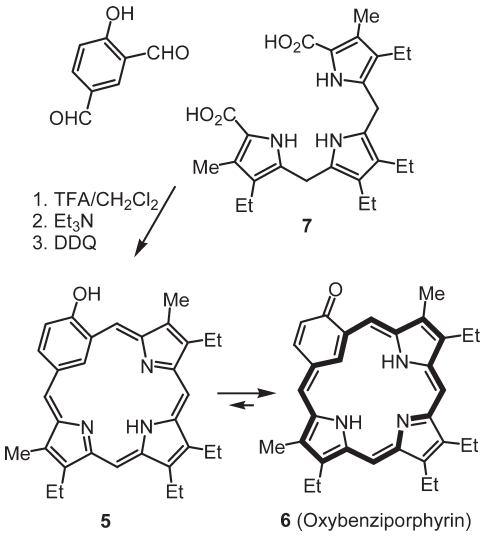

Scheme 2

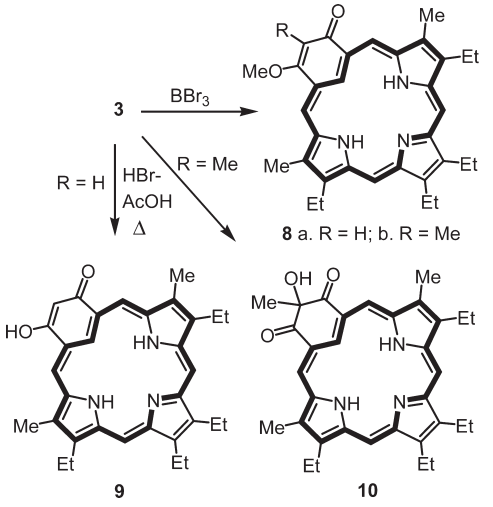

showed the 22-H upfield at −0.68 ppm, and even the 2-methyl analogue $\mathbf{3b}H_2^{2+}$ gave the 22-H resonance at a comparatively upfield value of 2.8 ppm.[10] In an early study, we speculated that 2-hydroxybenziporphrin **5** would tautomerize to give a fully aromatic system **6** with both a thermodynamically favorable carbonyl unit and a porphyrin-like delocalization pathway.[2] Reaction of 4-hydroxy-1,3-benzenedicarbaldehyde with tripyrrane **7** did indeed afford the aromatic carbaporphyrinoid **6**, named oxybenziporphyrin, and in this case, the internal CH was shifted to −7.2 ppm Scheme 1).[2,3] Treatment of dimethoxybenziporphyrins **3** with BBr_3 gave the methoxyoxybenziporphyrins **8**, while reaction of **3a** with refluxing HBr in acetic acid afforded a highly insoluble hydroxyoxybenziporphyrin **9** (Scheme 2).[10] However, cleavage of the methyl ethers in **3b** with refluxing HBr in acetic acid occurred with concomitant oxidation to afford the highly unusual benziporphyrin derivative **10**.[10] This system showed strikingly diatropic characteristics, and its proton NMR spectrum afforded a resonance for the 22-H at −8.52 ppm, while the external *meso*-protons gave rise to two 2H singlets at 9.39 and 10.19 ppm.[10] Given the unusual characteristics of this system, we were interested in the development

Scheme 3

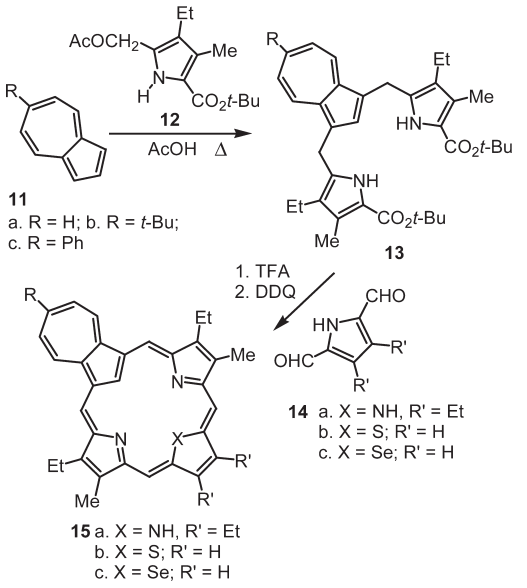

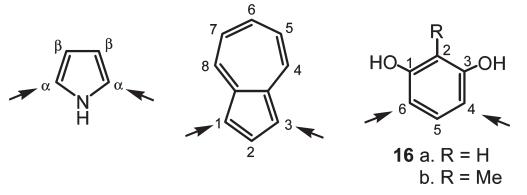

Figure 1. Favored sites for electrophilic substitution in pyrrole, azulene, and resorcinol.

of an alternative and more general route to this type of highly aromatic porphyrinoid. In other work, we had shown that azulenes **11** reacted with acetoxymethylpyrroles **12** in the presence of acetic acid to generate tripyrrane analogues **13** (Scheme 3).[18−20] Cleavage of the *tert*-butyl ester protective groups with TFA, followed by a "3 + 1" reaction with pyrrole dialdehyde **14a** and oxidation with DDQ afforded azuliporphyrins **15a**.[18−21] Heteroanalogues **15b** and **15c** were prepared similarly from thiophene and selenophene dialdehydes **14b** and **14c**.[18,19] In most porphyrin syntheses, the formation of oligopyrrolic intermediates and the macrocycles themselves relies on favorable electrophilic substitution at the α-positions on the pyrrole nucleus. The formation of azulitripyrranes **13** relies upon azulene's ability to undergo preferential electrophilic substitution at the structurally equivalent 1,3-positions (Figure 1),[18−20,22−24] and in this respect, azulene acts as a substitute for pyrrole in this chemistry. As resorcinol (**16a**) and 2-methylresorcinol (**16b**) also favor electrophilic substitution at the analogous 4,6-positions (Figure 1), we speculated that these dihydroxybenzenes could be used to prepare tripyrrane analogues as well. These benzitripyrranes (**17**) would in turn be potential intermediates for "3 + 1" MacDonald syntheses[25,26] of modified benziporphyrins like **10**.[27] The successful application of this strategy to the synthesis of benziporphyrin analogues is presented below.

RESULTS AND DISCUSSION

Azulitripyrrane **13a** was prepared by reacting azulene and acetoxymethylpyrrole **12** in refluxing acetic acid and isopropyl

Scheme 4

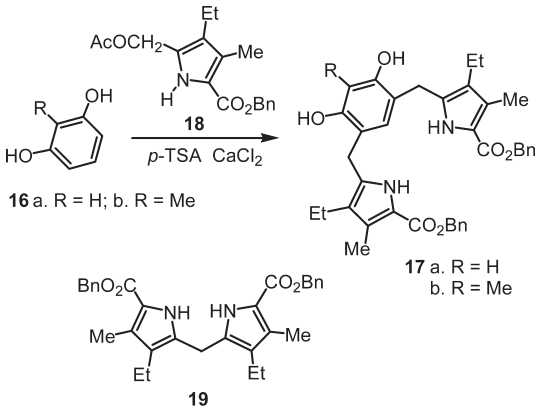

Scheme 5

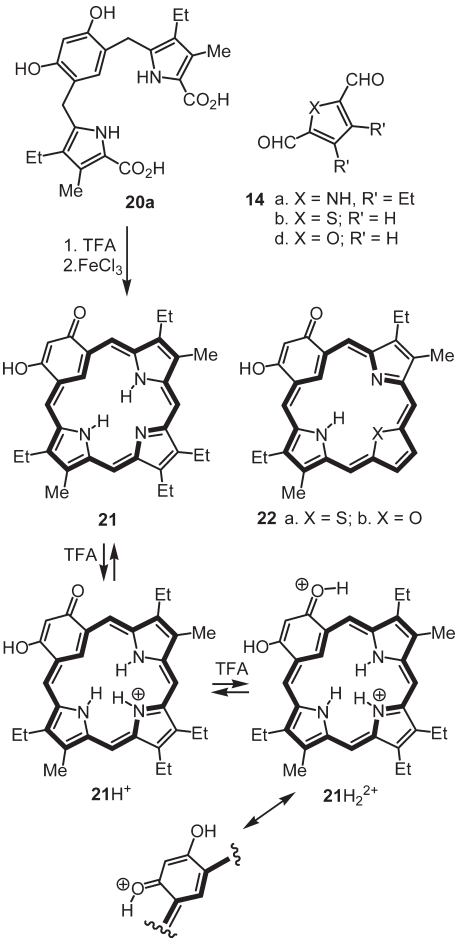

alcohol (Scheme 3),[18] and we initially anticipated that resorcinol could be reacted under the same conditions. However, when **16a** was reacted with 2 equiv of acetoxymethylpyrrole **18**, none of the targeted benzitripyrrane **17a** was formed (Scheme 4). Trace amounts of the desired product were identified when the reaction was carried out in refluxing acetic acid and ethanol. A problem that arises in this chemistry is that competing reactions can occur, specifically self-condensation of pyrrole **18** to give a dipyrrylmethane **19** and solvolysis reactions that can afford ether derivatives. In order to obtain practical yields of benzitripyrrane, electrophilic substitution of resorcinol must occur more rapidly than these competing processes. A series of experiments were conducted to optimize the reaction of resorcinol with **18**. Reaction of **16a** and **18** in acetic acid with Montmorillonite clay[28] gave **17a** in 6% yield. Montmorillonite clay gave better results in diethyl ether and generated **17a** in 15% yield. In dichloromethane, the yield was raised to 17%. Other types of acid catalysts were investigated, including Florisil, HBr, and methanesulfonic acid, but these all gave inferior results. As phenoxide ions are more reactive toward electrophiic substitution than phenols, reactions were attempted using basic conditions with sodium hydroxide, DBU, or DMAP, but only trace amounts of the benzitripyrrane product was formed. *p*-Toluenesulfonic acid in dichloromethane gave modest results (12% yield), but addition of calcium chloride with this acid catalyst raised the yield to 24% (Scheme 4). The role of the calcium chloride is unclear. It may act by absorbing trace amounts of water or as a cocatalyst. By itself, calcium chloride was not a useful catalyst. Reaction of **16a** and **18** in the presence of *p*-toluenesulfonic acid with other inorganic salts such as magnesium sulfate, sodium sulfate, or sodium chloride showed no improvement in the yields over using the acid catalyst alone. Self-condensation of the acetoxymethylpyrrole **18** to form dipyrrylmethane **19** was the main side reaction under these conditions. In an attempt to minimize this side reaction, a solution of **18** in dichloromethane was added over a 10 h period via a syringe pump to a stirred mixture of resorcinol, *p*-toluenesulfonic acid, and calcium chloride in dichloromethane. This modification gave the best results, and following chromatography on a silica column, benzitripyrrane **17** was isolated in 33% yield. The product fractions were identified by TLC. On the plate, the dipyrrylmethane byproduct turned red in the presence of bromine vapor,[29,30] but the benzitripyrrane gave a characteristic blue color.[30] Recrystallization from chloroform−hexanes gave **17** as white crystals. Under the same conditions, methylresorcinol **16b** was reacted with 2 equiv of acetoxymethylpyrrole **18**, and the related benzitripyrrane was isolated in 30% yield. Again, the product was purified by column chromatography on silica, and the product fractions were identified by TLC. The tripyrrane analogue showed up as a dark green spot on the TLC plate in the presence of bromine vapor.

The benzitripyrranes were generated with terminal benzyl ester protective groups, and these were easily cleaved to give the corresponding dicarboxylic acids **20** in near-quantitative yields by treating **17** with hydrogen over 10% palladium−charcoal. Benzitripyrrane dicarboxylic acid **20a** was reacted with pyrrole dialdehyde **14a**[31] in the presence of TFA in dichloromethane for 16 h (Scheme 5). Following oxidation with dilute aqueous ferric chloride solution,[32] purification by flash chromatography on silica and recrystallization from chloroform−hexanes, hydroxyoxybenziporphyrin **21** was isolated in 37% yield. The UV−vis spectrum for **21** in 2% triethylamine−chloroform was very porphyrin-like with a strong Soret band at 422 nm, followed by four smaller Q bands at 528, 570, 620, and 684 nm (Figure 2). However, the free base in deacidified chloroform gave a very poor quality spectrum with a Soret band at 425 nm because of its very low solubility in this solvent (Figure 2). The spectrum in $Et_3N-CHCl_3$ was attributed to the formation of an anionic species (Figure 3). The UV−vis spectrum in 2% DBU−$CHCl_3$ was quite different, showing a broad Soret band at 409 nm as well as Q bands at 519, 559, 616, and 678 nm (see the Supporting

dx.doi.org/10.1021/jo201098c |J. Org. Chem. 2011, 76, 6295–6308

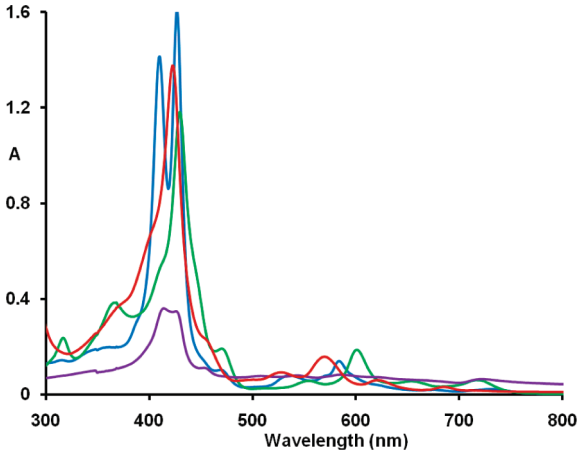

Figure 2. UV−vis spectra of hydroxyoxybenziporphyrin **21**. Free base in deacidified chloroform (purple line); monocation $\mathbf{21}H^+$ in $CHCl_3$ with 3 equiv of TFA (blue line); dication $\mathbf{21}H_2^{2+}$ in $CHCl_3$ with 200 equiv of TFA (green line); monoanion in 2% Et_3N−$CHCl_3$ (red line).

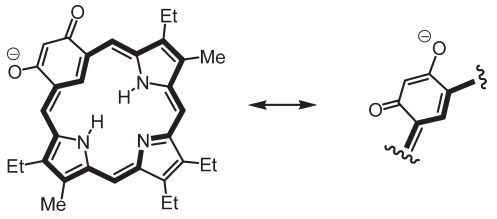

Figure 3. Monoanion formed by adding triethylamine to a solution of **21** in chloroform.

Information), and this may be due to further deprotonation of the system. Titration of a solution of **21** in chloroform with TFA initially generated a monocation $\mathbf{21}H^+$ (Scheme 5), and this showed a split Soret band at 410 and 427 nm (Figure 2). Monoprotonation was complete following the addition of 3 equiv of TFA, but further addition of acid generated the dication $\mathbf{21}H_2^{2+}$ (Scheme 5). The system was fully diprotonated in the presence of 200 equiv of TFA. The dication gave a Soret band at 429 nm and Q bands at 555, 601, 653, and 717 nm. Further addition of TFA resulted in minor changes in the UV−vis spectrum (see the Supporting Information). As porphyrinoid **21** is poorly soluble in organic solvents and the free base could not be characterized by proton NMR spectroscopy. However, the dication in TFA−$CDCl_3$ gave a well-resolved proton NMR spectrum that showed the internal CH at −2.35 ppm and a broad NH near −0.8 ppm. The external *meso*-protons gave two 2H singlets at 8.89 and 10.10 ppm. The methyl substituents, which are strongly deshielded in true porphyrins to 3.6 ppm, showed up as a 6H singlet at 3.11 ppm. These data confirm that the dication is strongly diatropic, although the diatropicity is somewhat reduced compared to porphyrins[33] or the free base form of oxybenziporphyrin **6**.[2] These results are in line with those previously obtained for the isomer **9** and related methoxybenziporphyrins **8**.[10] Benzitripyrrane **20a** was also reacted with thiophene dialdehyde **14b** and furan dialdehyde **14d** in an attempt to prepare the heterobenziporphyrins **22**. The UV−vis spectra for these products were porphyrin-like and showed Soret bands near 400 nm. Unfortunately, these compounds were extremely insoluble in organic solvents even in the presence of

Scheme 6

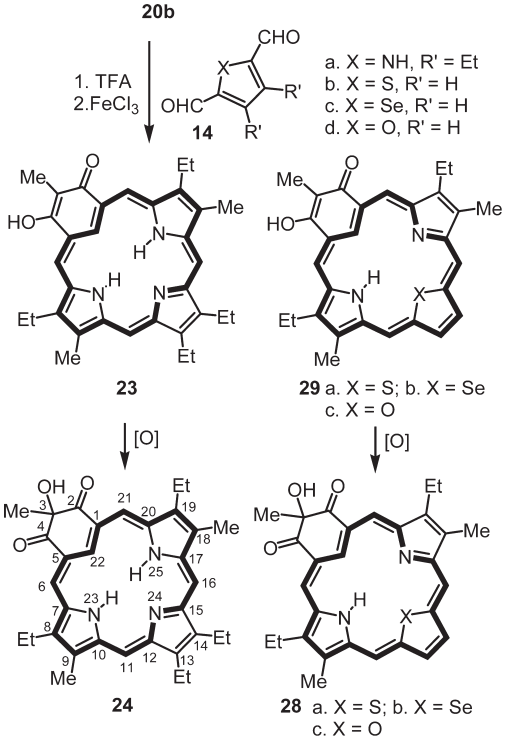

TFA and could not be characterized by NMR spectroscopy. High-resolution mass spectrometry confirmed that **22a** and **22b** had been generated, but it was not possible to obtain any further characterization or to determine the purity of the isolated materials.

Benzitripyrrane **20b** reacted with pyrrole dialdehyde **14a** under the same conditions, and following column chromatography and recrystallization, hydroxyoxybenziporphyrin **23** was isolated as the major product in 27% yield (Scheme 6). The further oxidized derivative **24** was observed as a minor byproduct (5%). Porphyrinoid **23** gave a porphyrin-like UV spectrum with a Soret band at 424 nm. The free base was again poorly soluble in chloroform, but the dication $\mathbf{23}H_2^{2+}$ formed upon addition of TFA gave a good quality proton NMR spectrum where the internal CH gave an upfield resonance at −1.14 ppm, while the *meso*-protons appeared downfield at 8.54 and 9.72 ppm. The diamagnetic ring current for $\mathbf{23}H_2^{2+}$ is slightly reduced compared to $\mathbf{21}H_2^{2+}$. The hydroxyl group helps to stabilize the positive charges without disrupting the 18π electron delocalization pathway that is responsible for the macrocycles aromatic properties (Scheme 7). The protonated form of oxybenziporphyrin ($\mathbf{6}H_2^{2+}$) shows a much greater decrease in diatropicity because of cross-conjugated phenolic canonical forms like **25**, and its proton NMR spectrum in TFA−$CDCl_3$ shows the 22-H at 1.5 ppm.[3a] The hydroxyl group in $\mathbf{23}H_2^{2+}$ is less effective at stabilizing the positive charges compared to $\mathbf{21}H_2^{2+}$ because of steric crowding by the methyl group, which disrupts conjugation in this portion of the molecule.

Isolation of pure **23** proved to be difficult because of its poor stability. In part, this was due to air oxidation to **24**, but this process was not very efficient. Significant conversion occurred when chloroform solutions of **23** were stirred open to the air for several days. However, only poor yields of **24** could be isolated.

dx.doi.org/10.1021/jo201098c |*J. Org. Chem.* 2011, 76, 6295–6308

Scheme 7

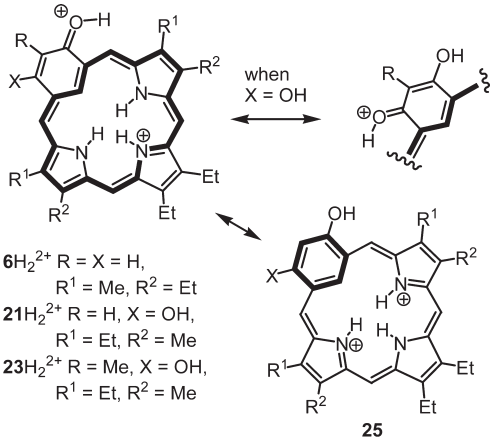

Scheme 8

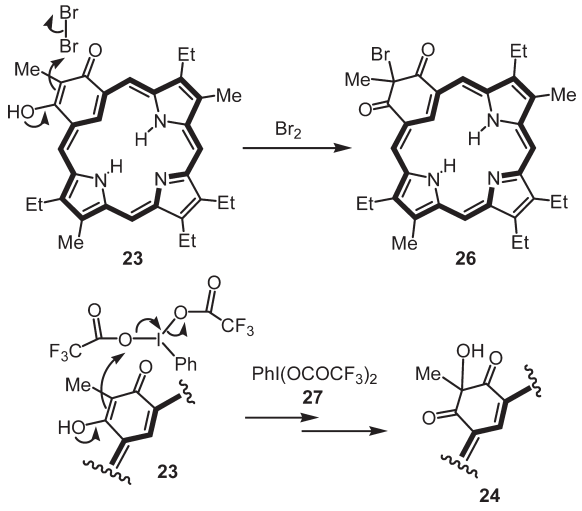

As porphyrinoid systems like **24** were the main target for this study, a range of oxidation conditions were considered. Oxidizing agents such as *tert*-butyl hydroperoxide, hydrogen peroxide, bleach, pyridine *N*-oxide, manganese dioxide, pyridinium chlorochromate, ferric chloride, iron(III) sulfate, iron(III) nitrate, and air were examined, but most of these trials led to decomposition. The best results were obtained by dissolving **23** in acetic acid with 5 equiv of ferric chloride and bubbling air through the stirred solution overnight. Following extraction, chromatography, and recrystallization from chloroform−methanol, **24** was isolated in 23% yield. However, even taking into account the quantity of **24** generated in the original condensation, the total yield of **24** from benzitripyrrane **20b** was only 11%.

Hydroxyoxybenziporphyrin **23** was also reacted with 1 equiv of bromine in acetic acid. This led to a straightforward electrophilic substitution to afford the bromo derivative **26** (Scheme 8). Following extraction, chromatography, and recrystallization from chloroform−hexanes, **26** was isolated as brown crystals in 44% yield. The UV−vis spectrum for the free base form of **26** gave a strong Soret band at 400 nm. On addition of TFA, the resulting cation **26**H^+ gave a split Soret band at 411 and 426 nm, together with a series of Q bands between 500 and 600 nm. The

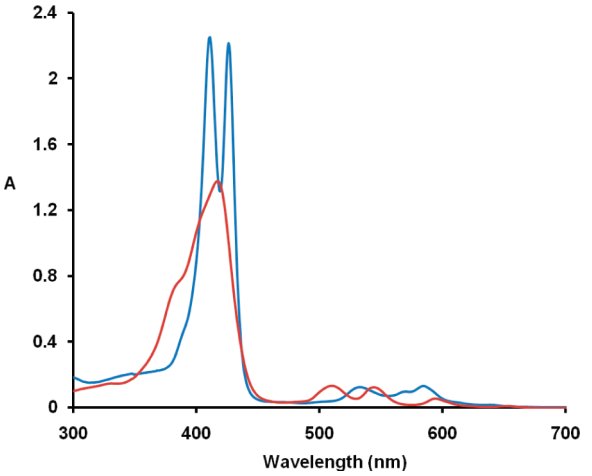

Figure 4. UV−vis spectra of oxidized benziporphyrin **24**. Free base in 1% Et_3N−$CHCl_3$ (red line). Cation **24**H^+ in 1% TFA−$CHCl_3$ (blue line).

proton NMR spectrum for **26** in $CDCl_3$ showed the internal CH at −7.45 ppm, while the exterior *meso*-protons gave rise to two 2H singlets at 9.72 and 10.58 ppm. The carbon-13 NMR spectrum for **26** confirmed the presence of a plane of symmetry for the macrocycle and showed a carbonyl resonance at 194.5 ppm.

As bromine addition to **23** occurs readily, we speculated that a similar electrophilic addition could give superior yields of porphyrinoid **24**. This was accomplished by reacting **23** with the hypervalent iodine reagent [bis(trifluoroacetoxy)iodo]-benzene (**27**, Scheme 8). Reaction of crude **23** with **27** in acetic acid gave slightly improved yields compared to the ferric chloride oxidation, but these yields remained disappointing. However, when the reaction was carried out in a mixture of dichloromethane and methanol in the presence of potassium carbonate, the oxidized benziporphyrin could be isolated as red crystals in an overall yield of 24% from benzitripyrrane **20b**. As expected, **24** gave a porphyrin-like UV−vis spectrum with broad Soret band at 417 nm and a series of Q bands in the visible region (Figure 4). Addition of TFA gave the corresponding cation **24**H^+ with a split Soret band at 413 and 427 nm (Figure 4). In fact, the spectroscopic properties for **24** and bromo derivative **26** are quite similar, which is hardly surprising given that they essentially share the same chromophore. The IR spectrum of **24** gave rise to two strong absorption bands at 1661 and 1699 cm^{-1} caused by the antisymmetrical and symmetrical stretching modes for the two carbonyl groups. The proton NMR spectrum for **24** in $CDCl_3$ showed the internal CH at −8.0 ppm (as is the case for all of these porphyrin analogues, the chemical shifts varied to a small extent with concentration), while the *meso*-protons appeared downfield as two 2H singlets at 9.50 and 10.31 ppm (Figure 5). The methyl groups gave a 6H singlet at 3.53 ppm, confirming the highly diatropic nature of porphyrinoid **24**. The methylene protons for the ethyl substituents are diastereotopic even though **24** has a plane of symmetry and is achiral. This is due to the two methylene protons residing in different environments relative to the tertiary alcohol unit. Figure 6 shows how free rotation about the benziporphyrin−CH_2 bond does not average out the environments for the individual protons (labeled H_A and H_B). The carbon-13 NMR spectrum of **24** again showed that the macrocycle possesses a plane of symmetry and the carbonyl units gave

dx.doi.org/10.1021/jo201098c |*J. Org. Chem.* 2011, 76, 6295–6308

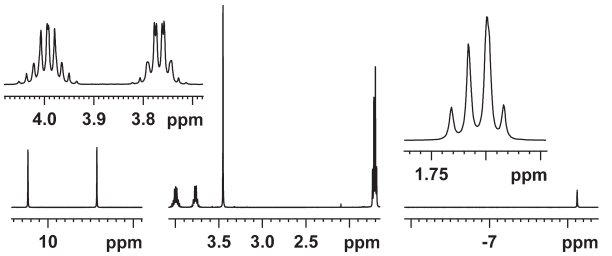

Figure 5. 500 MHz proton NMR spectrum of **24** in $CDCl_3$. The internal CH shows up beyond −8 ppm, while the *meso*-protons appear downfield at 9.5 and 10.3 ppm. The CH_2 units of the ethyl substituents also appear to be diastereotopic. Note that the methyl group on the tertiary alcohol overlaps with the two triplets for the ethyl substituents.

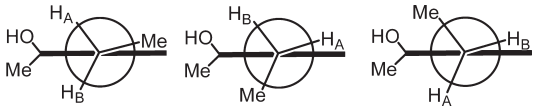

Figure 6. Free rotation of the ethyl substituent does not average out the environment for the two methylene protons H_A and H_B. The bold line represents a side view of benziporphyrinoid system **24**, and the methyl and hydroxyl units for the tertiary alcohol moiety differentiate between the two faces of the macrocycle. Each consecutive Newman projection represents a 120° rotation about the benziporphyrin−CH_2 bond. The same analysis also applies to structures **26**, **28**, and **30**.

rise to a signal at 201.4 ppm. In TFA−$CDCl_3$, the proton NMR spectrum for cation **24**H^+ showed the internal CH at −6.4 ppm, the NH resonances at −5.67 (1H) and −2.76 ppm (2H), and the *meso*-protons downfield at 10.17 (2H) and 10.88 ppm (2H). Again, the methyl groups gave a downfield singlet at 3.56 ppm.

Condensation of tripyrrane analogue **20b** with thiophene, selenophene, and furan dialdehydes **14b**−**d**, followed by oxidation with **27**, all gave heterobenziporphyrinoids **28** (Scheme 6). Reaction of **14d** with **20b** initially gave a mixture of **29c** and **28c** which was partially purified by chromatography. Oxidation of the mixture with 0.5 equiv of **27** in the presence of potassium carbonate was carried out with cooling in an ice bath. The reaction occurred very rapidly and was complete in approximately 3 min. Prolonged reaction times led to decomposition. The reaction solution was immediately washed with water, and the products were purified by column chromatography. Following recrystallization from chloroform−hexanes, **28c** was isolated in 20% yield. Using the ferric chloride conditions, this product could only be isolated in 6% yield. Thiophene dialdehyde **14b** similarly reacted with **20b** to give a mixture of **28a** and **29a**. This mixture was further oxidized with 0.5 equiv of **27** in the presence of potassium carbonate for 20 min. Following workup, purification by column chromatography, and recrystallization from chloroform−hexanes, the oxidized thiabenziporphyrin **28a** was isolated in 19% yield. This compares to an 8% yield using the ferric chloride conditions. Selenophene dialdehyde **14c** similarly reacted with tripyrrane analogue **20b** to give an analogous mixture of porphyrinoids **28b** and **29b**. However, oxidation with **27** was less successful in this case. The oxidized form **28b** was isolated in 8% yield together with crude **29b** in 24% yield. Nevertheless, the ferric chloride oxidation conditions only gave a trace amount of this oxidation product.

The UV−vis spectrum for 24-oxaporphyrinoid **28c** in Et_3N−$CHCl_3$ gave a Soret band at 426 nm and a series of Q

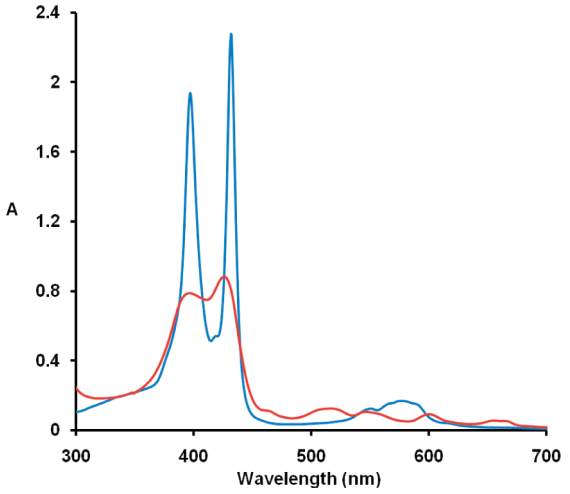

Figure 7. UV−vis spectra of oxabenziporphyrin **28c**. Free base in 1% Et_3N−$CHCl_3$ (red line). Cation **28c**H^+ in 1% TFA-$CHCl_3$ (blue line).

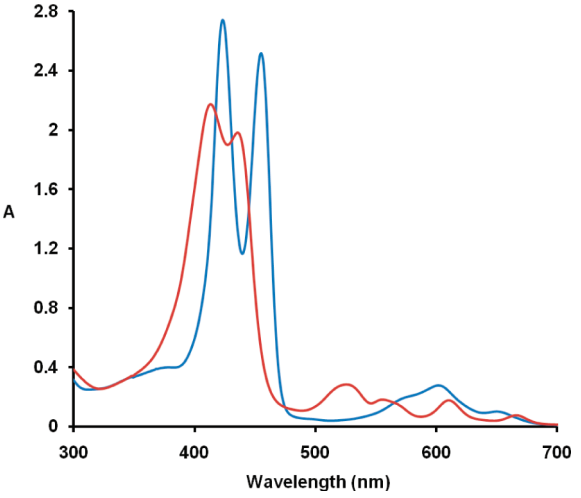

Figure 8. UV−vis spectra of thiabenziporphyrin **28a**. Free base in 1% Et_3N−$CHCl_3$ (red line). Cation **28a**H^+ in 1% TFA−$CHCl_3$ (blue line).

bands between 500 and 670 nm (Figure 7). As was the case of the related aza-version **24**, the cation **28c**H^+ in TFA−$CHCl_3$ gave a split Soret band at 397 and 432 nm, as well as a series of Q bands in the visible region (Figure 7). The Soret bands were comparatively sharp in this case. The proton NMR spectrum for **28c**H^+ in TFA−$CDCl_3$ showed the internal CH resonance at −6.92 ppm, the NHs at −3.47 ppm, and the *meso*-protons at 10.50 and 11.06 ppm. The methyl resonance appeared at 3.65 ppm. These data show that the monocation is highly diatropic and comparable to **24**H^+. The carbon-13 NMR spectrum showed 16 resonances, confirming the plane of symmetry for this macrocycle, and the carbonyl resonances were observed at 202.1 ppm. Thiabenziporphyrinoid **28a** also gave a porphyrin-like UV−vis spectrum with a broad split Soret band at 413 and 436 nm and Q bands at 526, 555, 609, and 665 nm (Figure 8). In TFA−$CHCl_3$, a split Soret band is observed at 423 and 454 nm together with a weaker band at 601 nm (Figure 8). In the proton NMR spectrum, the internal CH gave a resonance at −6.52 ppm, while the *meso*-protons appeared at 10.49 and 10.63 ppm (Figure 9). The

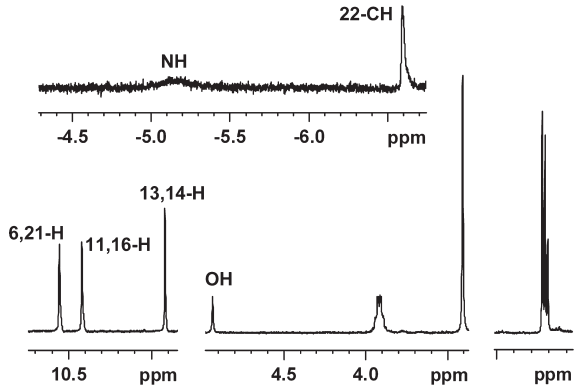

Figure 9. 500 MHz proton NMR spectrum of thiabenziporphyrin **28a** in $CDCl_3$.

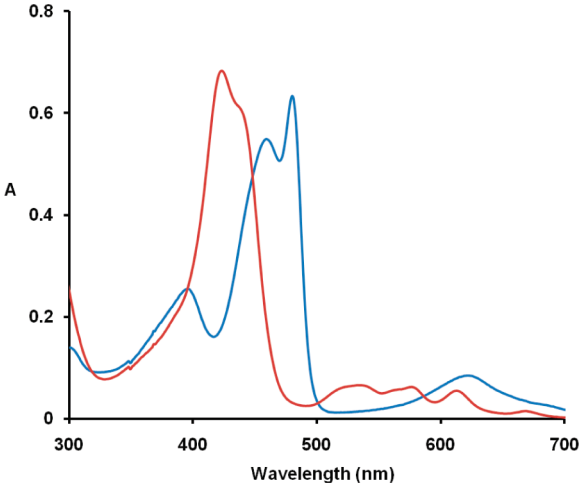

Figure 10. UV−vis spectra of selenabenziporphyrin **28b**. Free base in 1% Et_3N−$CHCl_3$ (red line). Cation **28b**H^+ in 1% TFA−$CHCl_3$ (blue line).

external thiophene protons were also downfield at 9.99 ppm, while the methyl protons resonated at 3.48 ppm. Cation **28a**H^+ in TFA−$CDCl_3$ showed the 22-H at −6.68 ppm, the NH protons at −3.77 ppm, the methyl groups at 3.68 ppm, the thiophene protons at 10.34 ppm, and the *meso*-protons at 11.11 and 11.22 ppm. Hence, thiabenziporphyrin **28a** retains highly diatropic characteristics for both the free base and cationic forms. Selenabenziporphyrin **28b** gave a porphyrin-like UV−vis spectrum with a Soret band at 423 nm (Figure 10), although the bands were broader and less intense than the UV−vis spectra of **24** or **28a** (oxabenziporphyrin **28c** gave much sharper bands than any of the other porphyrinoids). Similarly, the absorption bands for **28b**H^+ in TFA−$CHCl_3$ were also relatively broadened (Figure 10). The proton NMR spectrum for **28b** in $CDCl_3$ showed resonance for the 22-H at −6.36 ppm, the methyl resonance at 3.42 ppm, the selenophene protons at 10.16 ppm, and the *meso*-protons at 10.55 and 10.58 ppm. In TFA−$CDCl_3$, the internal CH appeared at −5.87 ppm, the NH protons were observed at −3.62 ppm, the methyl groups gave a 6H singlet at 3.65 ppm, the selenophene protons were present at 10.26 ppm, and the *meso*-protons showed up at 11.17 ppm. Although the presence of a large selenium atom in the macrocyclic cavity might be expected to decrease the planarity of this system, the

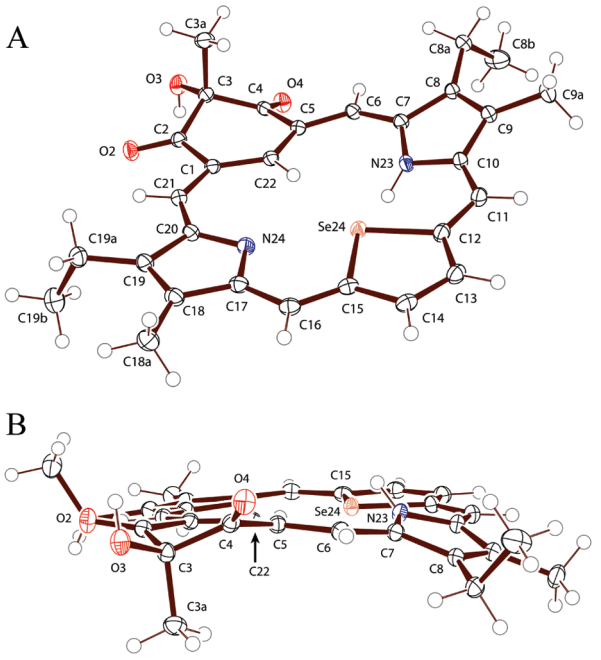

Figure 11. Color ORTEP III drawings (50% probability level, hydrogen atoms drawn arbitrarily small) of **28b·MeOH**. (A) General view. (B) Side view depicting the overall framework planarity with the NH pyrrole inclined 21° from main macrocyclic plane. Selected bond lengths (Å): C(1)−C(2) 1.493(2), C(2)−C(3) 1.535(2), C(3)−C(4) 1.523(2), C(4)−C(5) 1.492(2), C(5)−C(22) 1.418(2), C(22)−C(1) 1.409(2), C(5)−C(6) 1.411(2), C(6)−C(7) 1.391(2), C(7)−C(8) 1.437(2), C(8)−C(9) 1.386(2), C(9)−C(10) 1.424(2), C(10)−C-(11) 1.401(2), C(11)−C(12) 1.387(2), C(12)−C(13) 1.421(2), C-(13)−C(14) 1.372(2), C(14)−C(15) 1.423(2), C(15)−C(16) 1.380(2), C(16)−C(17) 1.406(2), C(17)−C(18) 1.458(2), C(18)−C-(19) 1.363(2), C(19)−C(20) 1.478(2), C(20)−C(21) 1.394(2), C-(21)−C(1) 1.409(2), C(7)−N(23) 1.377(2), N(23)−C(10) 1.384(2), C(12)−Se(24) 1.895(2), Se(24)−C(15) 1.870(2), C(17)−N(25) 1.358(2), N(25)−C(20) 1.365(2).

macrocycle retains highly diatropic characteristics. The carbon-13 NMR spectra for **28a** and **28b** in TFA−$CDCl_3$ again confirm that the macrocycles possess planes of symmetry and show the carbonyl resonances at 202.1 and 200.9 ppm, respectively. Spectroscopic data were also obtained for **29b**, although it was contaminated with a small amount of **28b**. The UV−vis spectrum for **29b** showed a Soret band at 425 nm and Q bands at 534, 564, 606, and 720 nm. The proton NMR spectrum for **29b**H^+ in TFA−$CDCl_3$ showed the internal CH at −0.91 ppm, the methyl resonance at 3.06 ppm, the selenophene protons at 9.25 ppm, and the *meso*-protons at 9.61 and 10.25 ppm.

The X-ray crystal structure of the free base selenabenziporphyrinoid has also been obtained as the methanol solvate **28b·MeOH** (Figure 11). This not only confirms the presence of a selenophene moiety but also demonstrates that one pyrrole moiety must turn out of the main macrocyclic plane to accommodate the large Se atom, as evidenced by the 21° incline of the plane of the NH containing pyrrole relative to the main framework plane defined as the macrocyclic carbon atoms excluding the NH pyrrole, the two carbonyls, and alcohol C atoms. The β C atoms of the NH pyrrole are significantly displaced about 0.7 Å above the framework plane. The sp^3 C atom is 0.32 Å above the plane. In contrast, the selenophene, the pyrrolenine unit, and the carbocyclic ring excluding the sp^3 carbon are fairly coplanar, and

dx.doi.org/10.1021/jo201098c |*J. Org. Chem.* 2011, 76, 6295–6308

Scheme 9

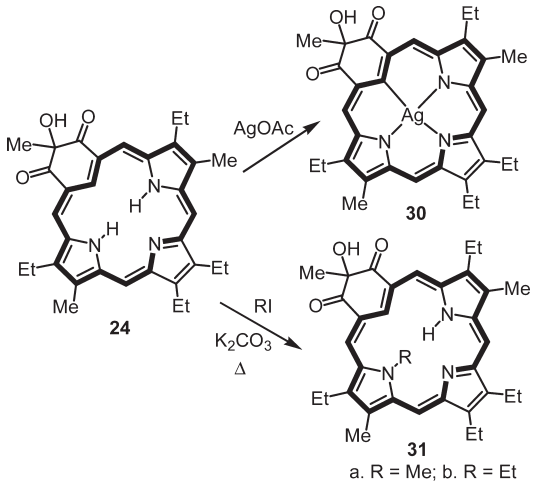

the framework atoms have an rms deviation from their plane equal to only 0.077 Å. A space-filling diagram reveals that the large Se atom makes it quite crowded in the center of the ring, which seems sufficient to justify the NH pyrrole deviating from planarity. In the solid-state structure, the NH H atom is best modeled based on residual electron density in the difference Fourier map and is found to be atypically bent away from the pyrrole plane. This may in part be due to the solid-state packing arrangement in which pairs of **28b** molecules appear to be conjoined across a crystallographic inversion center via weak NH···N hydrogen-bonding interactions. However, the 3.344(2) Å N−N separation is rather large, so the apparent location of this hydrogen atom may simply be due to spatial overcrowding within the macrocycle. The related system 5,20-diphenyl-10,15-di-*p*-tolyl-21-selenaporphyrin, which contains only one internal H atom, contains a very planar framework,[34] while N-confused 5,20-di-*p*-tolyl-10,15-diphenylthiaporphyrin, which contains an S atom and two internal H atoms like **28b**, displays a significantly saddled structure.[35] However, care must be taken to avoid exaggerating the correlation between planarity and apparent internal macrocyclic crowding. A related N-confused pyriporphyrin, 6,21-diphenyl-11,16-di-*p*-tolyl-3-aza-24-thiabenziporphyrin, has a saddled framework conformation, yet only possesses a single internal H atom.[36] In fact, analysis of the 2010 Cambridge Structural Database showed that the 15 previously reported X-ray structural characterizations of monothiaporphyrins and monoselenaporphyrins[37] lack clear trends in solid state macrocyclic planarity. The structure also shows the six-membered ring methyl unit in a pseudoaxial orientation, while the hydroxyl group is pseudoequatorial. This may be due to favored hydrogen bonding with the methanol solvate within the crystal lattice.

Many carbaporphyrinoid systems, including N-confused porphyrins,[38] oxybenziporphyrins,[13,39] oxynaphthiporphyrins,[13,39] benzocarbaporphyrins,[40] and tropiporphyrins,[41] act as trianionic ligands and readily form silver(III) organometallic derivatives.[39] These porphyrin analogues all possess a CH NH N NH arrangement of core atoms.[42−44] As the core atoms in oxidized benziporphyrin **24** are arranged in the same way, we anticipated that a similar organometallic derivative could be prepared for this species. Silver(I) acetate was stirred with **24** in a mixture of methanol and dichloromethane for 16 h (Scheme 9). Flash chromatography on silica afforded a dark orange fraction, and subsequent recrystallization from chloroform−hexanes gave the expected silver(III) complex **30** in 87% yield. In the proton NMR spectrum for **30**, the *meso*-protons were observed at 9.19 and 9.91 ppm and the methyl substituents gave rise to a resonance at 3.32 ppm, confirming that the complex retains most of its diatropic characteristics. The UV−vis spectrum for **30** gave a Soret band at 422 nm and three weaker Q bands between 500 and 600 nm. In 1% TFA−$CHCl_3$, the silver complex was rapidly demetalated and the UV−vis spectrum showed the formation of cation **24**H^+. Bromo derivative **26** was also reacted with silver acetate, but in this case only very low yields of a silver(III) complex was formed. Silver(I) cations have a high affinity for halogens and this appears to lead to side reactions involving loss of bromide ions.

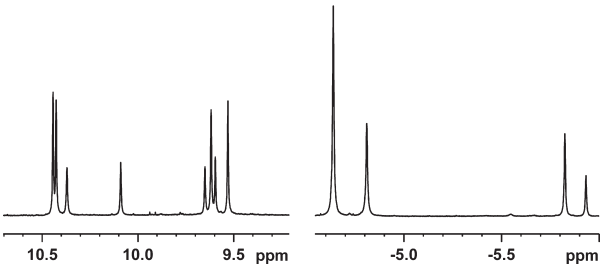

Figure 12. Partial 500 MHz proton NMR spectrum of 22-methylbenziporphyrin **31a** in $CDCl_3$ showing the presence of two different diastereomers. Each diastereomer gives rise to four different singlets for the *meso*-protons between 9.5 and 10.5 ppm. In addition, two singlets for the internal methyl groups can be seen near −4.7 ppm, while the 22-H peaks show up between −5.8 and −6.0 ppm.

Porphyrinoid **24** was also reacted with alkyl iodides to investigate the possibility of introducing *N*-alkyl substituents. Reaction of **24** with methyl iodide and potassium carbonate was carried out in refluxing acetone (Scheme 7). Following chromatography on silica, the product was collected as a dark purple fraction in 70% yield. The proton NMR spectrum showed that the product consisted on a mixture of two alkylation products in a ratio of approximately 2:1. Both products had four different resonances for the *meso*-protons and no longer showed the presence of a plane of symmetry (Figure 12). On the basis of these observations, the methyl substituent must have been introduced onto a pyrrolic unit next to the carbocyclic ring. As the methyl group is too large to pass through the central cavity, two diastereomers are possible where the alkyl substituent is either *cis* or *trans* to the peripheral OH group. The spectroscopic data did not allow us to identify which stereoisomer was favored. The methyl group does not undermine the diatropicity of this system. In the proton NMR spectrum for the mixture, the major diastereomer showed the internal CH at −5.73 ppm and the *N*-methyl at −4.54 ppm, while the *meso*-protons gave singlets at 9.62, 9.71, 10.52, and 10.54 ppm (Figure 12). The minor diastereomer gave the 22-H singlet at −5.84 ppm and the *N*-methyl resonance at −4.71 ppm, and the *meso*-protons appeared at 9.69, 9.74, 10.18, and 10.47 ppm (Figure 12). Reaction of **24** with ethyl iodide gave similar results, although in this case it was necessary to raise the temperature by using refluxing methyl ethyl ketone as the solvent. A mixture of two diastereomers, again in a ratio of approximately 2:1, was obtained in 67% yield, and the same regioselectivity was observed. The environment for the *N*-ethyl groups shows a high degree of chiral discrimination. In the proton NMR spectrum, the major diastereomer showed the

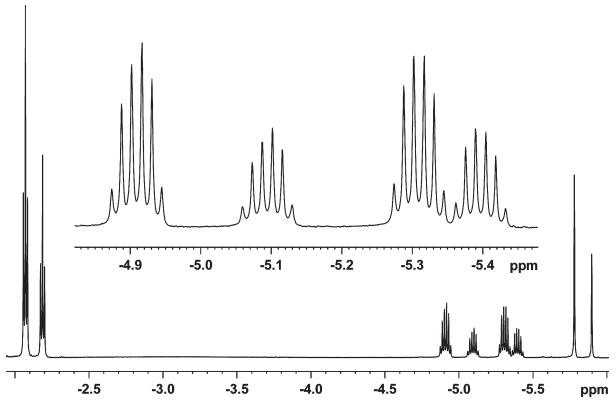

Figure 13. Partial 500 MHz proton NMR spectrum of 22-ethylbenziporphyrin **31b** in $CDCl_3$ showing details of the upfield region. Two diastereomers are present that give two sets of peaks for the internal ethyl substituents and the 22-Hs. The methylene protons are highly diastereotopic, demonstrating that they lie in a stereochemically discriminating region for these chiral derivatives.

internal methylene protons as two 1H multiplets at −5.3 and −4.9 ppm, showing that the two diastereotopic protons reside in significantly different environments (Figure 13). The strongly diatropic nature of the macrocycle was confirmed by the presence of the 22-H resonance at −5.76 ppm and the presence of four downfield singlets for the *meso*-protons at 9.70, 9.71, 10.53, and 10.61 ppm. Similar results were noted for the minor diastereomer, which again showed strongly differentiated methylene proton resonances for the internal ethyl group at −5.41 and −5.11 ppm. Both diastereomers consist of a pair of enantiomers, and this system therefore shows potential in the design of chiral catalysts.[45]

CONCLUSION

Tripyrrane analogues have been prepared from resorcinol and 2-methylresorcinol and used as intermediates in the synthesis of hydroxyoxybenziporphyrins and further oxidized derivatives. The initial products derived from the reaction of the methylresorcinol-derived tripyrrane analogue with pyrrole, furan, thiophene, or selenophene dialdehydes were unstable, but further oxidation with [bis(trifluoroacetoxy)iodo]benzene gave highly diatropic benziporphyrins with porphyrin-like UV−vis spectra. These results show that modified benziporphyrins can be highly aromatic systems even though simple benziporphyrins are usually considered to be devoid of macrocyclic aromatic properties. An oxidized benziporphyrin was shown to readily form a silver(III) derivative and also underwent a regioselective alkylation to give mixtures of chiral diastereomers. The unusual characteristics of these carbaporphyrinoids suggest that the full potential of benziporphyrin systems remains to be discovered.[46]

EXPERIMENTAL SECTION

4,6-Bis(5-benzyloxycarbonyl-3-ethyl-4-methyl-2-pyrrolylmethyl)-1,3-dihydroxybenzene (17a). A solution of benzyl 5-acetoxymethyl-4-ethyl-3-methylpyrrole-2-carboxylate[47] (1.20 g, 3.81 mmol) in dichloromethane (70 mL) was added to a stirred mixture of resorcinol (0.20 g, 1.8 mmol), *p*-toluenesulfonic acid monohydrate (0.20 g), and calcium chloride (2.72 g) in dichloromethane (40 mL) in a 200 mL round-bottom flask over a 10 h period using a syringe pump. The resulting mixture was stirred for a further 6 h and then washed with water and saturated sodium bicarbonate solution. The solvent was removed under reduced pressure, and the resulting red residue was chromatographed on silica gel eluting with 15% ethyl acetate−toluene. The product was collected as an orange fraction. Recrystallization from chloroform−hexanes afforded the tripyrrane analogue (0.373 g, 0.602 mmol, 33%) as white crystals: mp 216−217 °C; ^{1}H NMR (500 MHz, DMSO-d_6) δ 0.70 (6H, t, J = 7.5 Hz), 2.10 (4H, q, J = 7.5 Hz), 2.11 (6H, s), 3.57 (4H, s), 5.20 (4H, s), 6.16 (1H, s), 6.34 (1H, s), 7.30 (2H, t, J = 7.1 Hz), 7.36 (4H, t, J = 7.4 Hz), 7.40 (4H, d, J = 7.3 Hz), 9.16 (2H, s), 10.69 (2H, s); ^{13}C NMR (DMSO-d_6) δ 10.4, 15.2, 16.7, 24.9, 64.3, 102.2, 115.6, 116.4, 123.1, 126.2, 127.7, 127.8, 128.5, 129.8, 133.6, 137.2, 153.3, 160.6; HRMS (FAB) calcd for $C_{38}H_{40}N_2O_6$ + H m/z 621.2965, found 621.2964. Anal. Calcd for $C_{38}H_{40}N_2O_6$: C, 73.53; H, 6.49; N, 4.51. Found: C, 73.66; H, 6.44; N, 4.53.

4,6-Bis(5-carboxy-3-ethyl-4-methyl-2-pyrrolylmethyl)-1,3-dihydroxybenzene (20a). In a hydrogenation vessel, the foregoing tripyrrane analogue (897 mg, 1.45 mmol) was dissolved in freshly distilled THF (150 mL) and methanol (50 mL), and the solution was purged with nitrogen. Then, 10% palladium−charcoal (200 mg) was added, and the resulting mixture was shaken under an atmosphere of hydrogen at 40 psi at room temperature overnight. The catalyst was filtered off and the solvent removed in vacuo to yield the dicarboxylic acid (0.632 g, 1.44 mmol, 99%) as pink crystals: mp 134−135 °C; ^{1}H NMR (400 MHz, DMSO-d_6) δ 0.75 (6H, t, J = 7.4 Hz), 2.11 (6H, s), 2.17 (4H, q, J = 7.4 Hz), 3.56 (4H, s), 6.37 (1H, s), 6.39 (1H, s), 9.24 (2H, s), 10.38 (2H, s), 11.72 (2H, br s); ^{13}C NMR (DMSO-d_6) δ 10.2, 15.4, 16.8, 25.2, 102.4, 116.6, 122.5, 125.1, 130.5, 132.6, 153.4, 162.4. Anal. Calcd for $C_{24}H_{28}N_2O_6$: C, 65.44; H, 6.41; N, 6.36. Found: C, 65.55; H, 6.52; N, 6.15.

4,6-Bis(5-benzyloxycarbonyl-3-ethyl-4-methyl-2-pyrrolylmethyl)-1,3-dihydroxy-2-methylbenzene (17b). A solution of acetoxymethylpyrrole **18**[47] (3.60 g, 11.4 mmol) in dichloromethane (80 mL) was slowly added over a 10 h period using a syringe pump to a stirred mixture of 2-methylresorcinol (0.720 g, 5.8 mmol), *p*-toluenesulfonic acid monohydrate (0.60 g), and calcium chloride (8.15 g) in dichloromethane (120 mL). The resulting mixture was stirred for a further 6 h and then washed with water and saturated sodium bicarbonate solution. The solvent was removed under reduced pressure and the resulting oily residue chromatographed on silica gel eluting with 10% ethyl acetate−toluene. The product was collected as an orange fraction. Recrystallization from chloroform−hexanes afforded the tripyrrane analogue (1.107 g, 1.75 mmol, 30%) as pink crystals: mp 161−163 °C; ^{1}H NMR (400 MHz, $CDCl_3$) δ 1.03 (6H, t, J = 7.4 Hz), 1.90 (3H, s), 2.27 (6H, s), 2.44 (4H, q, J = 7.6 Hz), 3.76 (4H, s), 5.24 (4H, s), 5.37 (2H, br s), 6.66 (1H, s), 7.27−7.38 (10H, m), 8.95 (2H, br s); ^{13}C NMR ($CDCl_3$) δ 8.6, 10.8, 15.7, 17.4, 27.3, 65.7, 111.4, 117.55, 117.60, 124.2, 127.4, 128.1, 128.7, 128.9, 132.2, 136.9, 151.6, 161.9; HRMS (FAB) calcd for $C_{39}H_{42}N_2O_6$ + H m/z 635.3121, found 635.3124. Anal. Calcd for $C_{39}H_{42}N_2O_6$: C, 73.79; H, 6.67; N, 4.41. Found: C, 73.43; H, 6.65; N, 4.47.

4,6-Bis(5-carboxy-3-ethyl-4-methyl-2-pyrrolylmethyl)-1,3-dihydroxy-2-methylbenzene (20b). Dibenzyl ester **17b** (1.022 g, 1.61 mmol) was dissolved in freshly distilled THF (150 mL) and methanol (50 mL) and the solution purged with nitrogen. Then, 10% palladium−charcoal (200 mg) was added and the resulting mixture shaken under an atmosphere of hydrogen at 40 psi at room temperature overnight. The catalyst was filtered off, and the solvent was removed in vacuo to yield the dicarboxylic acid (0.709 g, 1.56 mmol, 97%) as red crystals: mp 141−142 °C; ^{1}H NMR (500 MHz, DMSO-d_6) δ 0.75 (6H, t, J = 7.5 Hz), 2.04 (3H, s), 2.12 (6H, s), 2.13 (4H, q, J = 7.5 Hz), 3.62 (4H, s), 6.19 (1H, s), 8.09 (2H, s), 10.44 (2H, s), 11.66 (2H, v br); ^{13}C NMR (DMSO-d_6) δ 10.1, 10.3, 15.3, 16.8, 25.8, 112.5, 116.6, 118.3, 122.7, 125.3, 126.7, 132.2, 151.1, 162.5. Anal. Calcd for $C_{25}H_{30}N_2O_6$: C, 66.06; H, 6.65; N, 6.16. Found: C, 66.44; H, 7.14; N, 5.81.

8,13,14,19-Tetraethyl-4-hydroxy-9,18-dimethyl-2-oxybenziporphyrin (21). In a 100 mL pear-shaped flask, tripyrrane analogue **20a** (75.0 mg, 0.17 mmol) and TFA (1 mL) were stirred under nitrogen for 2 min. Dichloromethane (99 mL) was added, followed immediately by pyrrole dialdehyde **14a**[31] (30.5 mg, 0.17 mmol), and the resulting mixture was stirred overnight under nitrogen. The mixture was shaken vigorously with aqueous 0.1% w/v ferric chloride solution (100 mL) for 5 min, and the aqueous solution was then back-extracted with chloroform. The combined organic solutions were washed with water and 5% aqueous sodium bicarbonate solution, the solvent was removed under reduced pressure, and the resulting dark blue residue was chromatographed on flash silica eluting with 5% methanol−chloroform. The product was collected as a dark brown fraction. Recrystallization from chloroform−hexanes yielded the oxybenziporphyrin (31.3 mg, 0.063 mmol, 37%) as brown crystals: mp >300 °C; UV−vis (2% Et_3N−$CHCl_3$) λ_{max} ($\log_{10}\varepsilon$) 422 (5.08), 455 (sh, 4.30), 528 (3.91), 570 (4.14), 620 (3.72), 684 nm (3.44); UV−vis (2% DBU−$CHCl_3$) λ_{max} ($\log_{10}\varepsilon$) 409 (5.02), 519 (3.98), 559 (4.06), 616 (3.70), 678 nm (3.25); UV−vis (3 equiv TFA−$CHCl_3$) λ_{max} ($\log_{10}\varepsilon$) 410 (5.10), 427 (5.15), 471 (3.96), 535 (3.85), 569 (sh, 3.84), 584 (4.09), 730 nm (3.31); UV−vis (200 equiv TFA−$CHCl_3$) λ_{max} ($\log_{10}\varepsilon$) 316 (4.32), 368 (4.53), 429 (5.02), 470 (4.23), 555 (3.70), 601 (4.22), 653 (sh, 3.70), 717 nm (3.74); IR (KBr) 3440 (OH str.), 1611 (C═O str); ^{1}H NMR (500 MHz, TFA−$CDCl_3$) δ −2.35 (1H, s), −0.81 (1H, br s), 1.51 (6H, t, J = 7.7 Hz), 1.68 (6H, t, J = 7.7 Hz), 2.42 (2H, br s), 3.12 (6H, s), 3.62−3.71 (8H, m), 7.59 (1H, s), 8.89 (2H, s), 10.10 (2H, s); ^{13}C NMR (TFA−$CDCl_3$) δ 11.0, 16.4, 17.0, 19.4, 19.9, 94.1, 105.8, 117.0, 117.2, 117.3, 133.8, 138.4, 144.7, 144.8, 150.5, 151.3, 176.7; HRMS (EI) calcd for $C_{32}H_{35}N_3O_2$ + H 494.2808, found 494.2808. Anal. Calcd for $C_{32}H_{35}N_3O_2 \cdot {}^1/_4CHCl_3$: C, 73.99; H, 6.79; N, 8.02. Found: C, 73.96; H, 6.84; N, 7.88.

8,13,14,19-Tetraethyl-4-hydroxy-3,9,18-trimethyl-2-oxybenziporphyrin (23). Tripyrrane analogue **20b** (225.1 mg, 0.496 mmol) was stirred with TFA (3 mL) under nitrogen for 2 min. Dichloromethane (300 mL) was added, followed immediately by dialdehyde **14a**[31] (89.0 mg, 0.497 mmol), and the resulting mixture was stirred overnight under nitrogen. The mixture was washed with aqueous 0.1% ferric chloride solution (300 mL), water, and 5% sodium bicarbonate, back-extracting at each at stage with chloroform. The solvent was removed under reduced pressure and the resulting dark brown residue chromatographed on flash silica eluting with 1.7% methanol−chloroform. The crude product was collected as a dark brown fraction. The solvent was removed under reduced pressure and the resulting brown residue chromatographed on flash silica eluting with 50% dichloromethane−chloroform. Initially, **24** was collected as a red fraction. Recrystallization from chloroform−methanol yielded oxybenziporphyrin **24** (13.2 mg, 0.0252 mmol, 5%) as red crystals, mp >300 °C. A later brown fraction was collected and recrystallized from chloroform-hexanes to yield the porphyrin analogue **23** (68.2 mg, 0.134 mmol, 27%) as brown crystals: mp >300 °C; UV−vis (Et_3N−$CHCl_3$) λ_{max} ($\log_{10}\varepsilon$) 423 (5.05), 457 (sh, 4.29), 509 (3.84), 542 (3.90), 576 (4.06), 626 (3.57), 691 nm (3.29); UV−vis (1% TFA−$CHCl_3$) λ_{max} ($\log_{10}\varepsilon$) 412 (4.98), 427 (5.09), 555 (3.81), 603 (4.02), 627 (sh, 3.77), 688 nm (3.45); ^{1}H NMR (500 MHz, TFA−$CDCl_3$) δ −1.14 (1H, s), 1.44 (6H, t, J = 7.7 Hz), 1.60 (6H, t, J = 7.7 Hz), 2.48 (3H, s), 2.98 (6H, s), 3.18 (2H, br s), 3.49−3.56 (8H, m), 8.54 (2H, s), 9.72 (2H, s); ^{13}C NMR (TFA−$CDCl_3$) δ 8.4, 10.7, 15.9, 16.3, 19.2, 19.8, 93.9, 110.8, 114.0, 116.5, 118.7, 134.3, 139.2, 145.7, 147.2, 153.0, 153.4, 170.7; HRMS (EI) calcd for $C_{33}H_{37}N_3O_2$ 507.2886, found 507.2876.

8,13,14,19-Tetraethyl-3,4-dihydro-3-hydroxy-3,9,18-trimethyl-4-oxo-2-oxybenziporphyrin (24). Method A. The partially purified hydroxyoxybenziporphyrin **23** (54.1 mg, 0.107 mmol) was dissolved in acetic acid (60 mL) and placed in a 100 mL three-neck round-bottom flask. Five equivalents of ferric chloride (87.0 mg, 0.53 mmol) was added, and air was bubbled through the stirred mixture overnight. Chloroform was added and the mixture washed with water followed by saturated sodium bicarbonate. The solvent was evaporated under reduced pressure and the residue chromatographed on flash silica, eluting with 50% dichloromethane−chloroform. The product was collected as a red fraction. Recrystallization from chloroform−methanol yielded the porphyrin analogue (13.1 mg, 0.025 mmol, 23%; 11% total yield from **20b**) as red crystals: mp >300 °C; UV−vis (1% Et_3N−$CHCl_3$) λ_{max} ($\log_{10}\varepsilon$) 384 (sh, 4.90) 417 (5.11), 509 (4.14), 544 (4.08), 593 nm (3.75); UV−vis (1% TFA−$CHCl_3$) λ_{max} ($\log_{10}\varepsilon$) 411 (5.32), 426 (5.32), 533 (4.08), 569 (3.93), 584 nm (4.08); IR (KBr) 1699, 1661 cm^{-1} (C═O str); ^{1}H NMR (500 MHz, $CDCl_3$) δ −8.04 (1H, s), 1.76−1.81 (15H, overlapping singlet and triplets), 3.53 (6H, s), 3.81−3.88 (4H, m), 4.01−4.13 (4H, m), 9.50 (2H, s), 10.31 (2H, s); ^{1}H NMR (500 MHz, TFA−$CDCl_3$) δ −6.38 (1H, s), −5.67 (1H, s), −2.76 (2H, s), 1.51 (3H, s), 1.62 (6H, t, J = 7.7 Hz), 1.87 (6H, t, J = 7.7 Hz), 3.56 (6H, s), 4.00−4.16 (8H, m), 10.17 (2H, s), 10.88 (2H, s); ^{13}C NMR ($CDCl_3$) δ 11.2, 17.5, 18.5, 19.9, 20.0, 30.2, 86.2, 94.9, 103.2, 119.7, 120.1, 130.4, 131.3, 138.4, 143.5, 145.1, 154.3, 201.4; ^{13}C NMR (TFA−$CDCl_3$) δ 11.7, 16.7, 17.5, 20.0, 20.3, 28.7, 87.3, 94.2, 110.5, 121.0, 129.1, 134.6, 137.1, 139.0, 142.2, 143.6, 147.0, 203.4; HRMS (FAB) calcd for $C_{33}H_{37}N_3O_3$ + H 524.2913, found 524.2916. Anal. Calcd for $C_{33}H_{37}N_3O_3$: C, 75.69; H, 7.12; N, 8.02. Found: C, 75.42; H, 6.94; N, 8.05.

Method B. TFA (1 mL) was added to tripyrrane dicarboxylic acid **20b** (90.8 mg, 0.200 mmol) in a 100 mL pear-shaped flask and the mixture stirred under nitrogen for 2 min. Dichloromethane (99 mL) was added, following immediately by pyrrole dialdehyde **14a**[31] (35.8 mg, 0.200 mmol), and the resulting mixture stirred overnight under nitrogen. The mixture was shaken vigorously with aqueous 0.1% ferric chloride solution (100 mL) for 5 min and then washed with water and saturated sodium bicarbonate, back-extracting at each stage with chloroform. The solvent was removed under reduced pressure and the resulting brown residue chromatographed on a flash silica column with 1.7% methanol−chloroform. Porphyrinoids **23** and **24** were collected as brown and red fractions, respectively. Evaporation of the two fractions separately gave brown and red residues. Porphyrin analogue **23** was collected as the major fraction, and **24** was isolated as a minor product. Crude porphyrinoid **23** was dissolved in 15 mL of 50% methanol−dichloromethane. [Bis(trifluoroacetoxy)iodo]benzene (**27**) (35.5 mg, 0.08 mmol) and potassium carbonate (250 mg) were added to the stirred mixture, and the reaction was monitored by UV−vis spectroscopy (the reaction may take 30 min). The resulting solution was washed with water, back-extracting with chloroform, and following evaporation of the solvent, the crude product was obtained as a dark green solid. Flash chromatography, eluting with 50% dichloromethane−chloroform, gave **24** as a red fraction. Recrystallization from chloroform−methanol gave **24** (25.2 mg, 0.048 mmol, 24% overall yield from **20b**) as a red powder, mp >300 °C.

8,13,14,19-Tetraethyl-3,4-dihydro-3-hydroxy-3,9,18-trimethyl-4-oxo-24-oxa-2-oxybenziporphyrin (28c). TFA (1 mL) was added to tripyrranedicarboxylic acid **20b** (75.0 mg, 0.165 mmol) in a 100 mL pear-shaped flask and the mixture stirred under nitrogen for 2 min. Dichloromethane (100 mL) was added, followed immediately by furan dialdehyde **14d** (20.4 mg, 0.165 mmol), and the resulting mixture stirred overnight under nitrogen. The mixture was washed with aqueous 0.1% ferric chloride solution (100 mL), water, and saturated sodium bicarbonate, back-extracting at each stage with chloroform. The solvent was removed under reduced pressure and the resulting brown residue chromatographed on a flash silica column with 3% methanol−chloroform. Porphyrinoids **29c** and **28c** were collected as overlapping brown and red fractions. Evaporation of the combined fractions gave a brown residue, and this was dissolved in 10 mL of 50% methanol−dichloromethane and cooled in an ice bath. [Bis(trifluoroacetoxy)iodo]benzene (**27**)

(35.5 mg, 0.082 mmol) and potassium carbonate (250 mg) were added to the stirred mixture, and the reaction was monitored by UV−vis spectroscopy so that the reaction could be stopped as soon as the conversion was complete. This usually took no more than 3 min. The resulting solution was washed with water, back-extracting with chloroform, and following evaporation of the solvent the crude product was obtained as a brown solid. Flash chromatography, eluting with 2.5% methanol−chloroform, gave **28c** as a red fraction. Recrystallization from chloroform−hexane gave the product (15.1 mg, 0.032 mmol, 20%) as a brown powder: mp >300 °C; UV−vis (1% Et_3N−$CHCl_3$) λ_{max} ($\log_{10}\varepsilon$) 397 (4.75), 426 (4.80), 516 (3.95), 546 (3.88), 600 (3.82), 656 nm (3.59); UV−vis (1% TFA−$CHCl_3$) λ_{max} ($\log_{10}\varepsilon$) 397 (5.14), 432 (5.21), 550 (3.95), 576 nm (4.07); ^{1}H NMR (500 MHz, TFA−$CDCl_3$) δ −6.92 (1H, s), −3.47 (2H, br s), 1.50 (3H, s), 1.72 (6H, t, J = 7.7 Hz), 3.65 (6H, s), 4.10−4.24 (4H, m), 10.14 (2H, s), 10.50 (2H, s), 11.06 (2H, s); ^{13}C NMR (TFA−$CDCl_3$) δ 11.6, 17.2, 20.3, 28.4, 87.5, 95.6, 112.0, 122.7, 130.1, 131.1, 135.0, 136.8, 139.8, 147.4, 154.2, 202.1; HR MS (ESI) calcd for $C_{29}H_{28}N_2O_4$ + H 469.2127, found 469.2134. Anal. Calcd for $C_{29}H_{28}N_2O_4 \cdot 0.3CHCl_3$: C, 69.78; H, 5.65; N, 5.55. Found: C, 70.02; H, 5.72; N, 5.14.

8,19-Diethyl-3,4-dihydro-3-hydroxy-3,9,18-trimethyl-4-oxo-24-thia-2-oxybenziporphyrin (28a). TFA (1 mL) was added to dicarboxylic acid **20b** (75.0 mg, 0.165 mmol) in a 100 mL pear-shaped flask and the mixture stirred under nitrogen for 2 min. Dichloromethane (100 mL) was added, followed immediately by thiophene dialdehyde **14b** (23.1 mg, 0.165 mmol), and the resulting mixture stirred overnight under nitrogen. The mixture was washed with aqueous 0.1% ferric chloride solution (100 mL), water, and saturated sodium bicarbonate, back-extracting at each stage with chloroform. The solvent was removed under reduced pressure and the resulting green residue chromatographed on a flash silica column with 3% methanol−chloroform. Porphyrinoids **29a** and **28a** were collected as green fractions. Evaporation of the combined fractions gave a dark green residue, and this was dissolved in 15 mL of 50% methanol−dichloromethane and cooled in an ice bath. [Bis(trifluoroacetoxy)iodo]benzene (**27**) (35.5 mg, 0.082 mmol) and potassium carbonate (250 mg) were added to the stirred mixture, and the reaction was stopped after 20 min. The resulting solution was washed with water, back-extracting with chloroform, and following evaporation of the solvent, the crude product was obtained as a dark green solid. Flash chromatography, eluting with chloroform, gave **28a** as a green fraction. Recrystallization from chloroform−hexane gave the product (15.3 mg, 0.0316 mmol, 19%) as a green powder: mp >300 °C; UV−vis (1% Et_3N−$CHCl_3$) λ_{max} ($\log_{10}\varepsilon$) 413 (4.86), 436 (4.81), 526 (3.96), 555 (3.73), 609 (3.71), 665 nm (3.16); UV−vis (1% TFA−$CHCl_3$) λ_{max} ($\log_{10}\varepsilon$) 348 (4.10), 423 (5.04), 454 (5.00), 601 nm (4.00); ^{1}H NMR (500 MHz, $CDCl_3$) δ −6.52 (1H, s), −5.07 (1H, v br), 1.79 (6H, t, J = 7.7 Hz), 1.81 (3H, s), 3.48 (6H, s), 3.95−4.03 (4H, m), 5.00 (1H, s), 9.99 (2H, s), 10.49 (2H, s), 10.63 (2H, s); ^{1}H NMR (500 MHz, TFA−$CDCl_3$) δ −6.68 (1H, s), −3.77 (2H, br s), 1.58 (3H, s), 1.77 (6H, t, J = 7.7 Hz), 3.68 (6H, s), 4.11−4.24 (4H, m), 10.34 (2H, s), 11.11 (2H, s), 11.22 (2H, s); ^{13}C NMR (TFA−$CDCl_3$) δ 11.9, 17.1, 20.2, 28.4, 88.0, 109.4, 112.4, 125.2, 128.9, 136.4, 136.9, 138.5, 143.7, 146.6, 202.1; HRMS (ESI) calcd for $C_{29}H_{28}N_2O_3S$ + H 485.1899, found 485.1920. Anal. Calcd for $C_{29}H_{28}N_2O_3S \cdot {}^1/_{10}CHCl_3$: C, 70.39; H, 5.70; N, 5.64. Found: C, 70.32; H, 5.48; N, 5.64.

Reaction of Tripyrrane Analogue 20b with 2,5-Selenophenedicarbaldehyde 14c. TFA (1 mL) was added to benzitripyrrane dicarboxylic acid **20b** (75.0 mg, 0.165 mmol) in a 100 mL pear-shaped flask and the mixture stirred under nitrogen for 2 min. Dichloromethane (100 mL) was added, following immediately by selenophenedialdehyde **14c** (30.1 mg, 0.165 mmol), and the resulting mixture stirred overnight under nitrogen. The mixture was shaken vigorously with aqueous 0.1% ferric chloride solution (100 mL) for 5 min and then washed with water and saturated sodium bicarbonate solution, back-extracting at each stage with chloroform. The solvent was removed under reduced pressure and the resulting green residue chromatographed on a flash silica column eluting initially with chloroform, and then the polarity was gradually increased to 3% methanol−chloroform. Porphyrinoids **28b** and **29b** were collected as green and brown fractions. Evaporation of the two fractions separately gave dark green residues. Selenabenziporphyrin **29b** was collected as the major fraction (29.3 mg, 0.057 mmol, 35%), and **28b** was isolated as a minor product (1.0 mg, 0.0019 mmol, 1.2%).

Porphyrinoid **29b** (29.3 mg, 0.0568) was dissolved in 20 mL of 50% methanol−dichloromethane and cooled in an ice bath. [Bis(trifluoroacetoxy)-iodo]benzene (**27**) (35.5 mg, 0.082 mmol) and potassium carbonate (250 mg) were added to the stirred mixture, and the reaction was monitored by UV−vis spectroscopy (the reaction may take 30 min). The resulting solution was washed with water, back-extracting with chloroform, and following evaporation of the solvent, the crude product was obtained as a dark green solid. Flash chromatography, eluting with chloroform, gave **28b** as a green fraction. However, only partial conversion occurred, and **29b** was also obtained as a later fraction. Recrystallization of the individual products from chloroform−hexane gave **28b** (7.1 mg, 0.013 mmol, 9.4% overall) as a brown powder and **29b** (20.6 mg, 0.040 mmol, 25%) as a green powder.

8,19-Diethyl-4-hydroxy-3,9,18-trimethyl-24-selena-2-oxybenziporphyrin (29b): mp >300 °C; UV−vis (1% Et_3N−$CHCl_3$) λ_{max} ($\log_{10}\varepsilon$) 425 (4.86), 534 (3.99), 564 (3.97), 606 (3.96), 720 nm (3.61); UV−vis (1% TFA−$CHCl_3$) λ_{max} ($\log_{10}\varepsilon$) 394 (4.53), 478 (4.87), 519 (4.83), 627 nm (3.68); ^{1}H NMR (500 MHz, TFA−$CDCl_3$) δ −0.91 (1H, s), 1.57 (6H, t, J = 7.7 Hz), 2.56 (3H, s), 3.06 (6H, s), 3.64 (4H, q, J = 7.7 Hz), 9.25 (2H, s), 9.61 (2H, s), 10.25 (2H, s); ^{13}C NMR (TFA−$CDCl_3$) δ 9.1, 10.7, 16.3, 19.9, 114.0, 114.7, 118.3, 123.2, 134.9, 137.2, 142.9, 154.7, 155.8, 159.2, 173.7. HR MS (ESI) calcd for $C_{29}H_{28}N_2O_2Se$ + H 517.1394, found 517.1373.

8,19-Diethyl-3,4-dihydro-3-hydroxy-3,9,18-trimethyl-4-oxo-24-seleno-2-oxybenziporphyrin (28b): mp >300 °C; UV−vis (1% Et_3N−$CHCl_3$) λ_{max} ($\log_{10}\varepsilon$) 423 (4.91), 438 (sh, 4.86), 533 (3.89), 577 (3.87), 613 (3.81); UV−vis (1% TFA−$CHCl_3$) λ_{max} ($\log_{10}\varepsilon$) 395 (4.48), 459 (4.81), 480 (4.88), 622 nm (4.00); ^{1}H NMR (500 MHz, $CDCl_3$) δ −6.36 (1H, s), −5.1 (1H, v br), 1.76 (6H, t, J = 7.6 Hz), 1.80 (3H, s), 3.42 (6H, s), 3.88−3.97 (4H, m), 5.03 (1H, s), 10.16 (2H, s), 10.55 (2H, s), 10.58 (2H, s); ^{1}H NMR (500 MHz, TFA−$CDCl_3$) δ −5.87 (1H, s), −3.62 (2H, br s), 1.58 (3H, s), 1.79 (6H, t, J = 7.7 Hz), 3.65 (6H, s), 4.10−4.23 (4H, m), 10.26 (2H, s), 11.17 (4H, s); ^{13}C NMR (TFA−$CDCl_3$) δ 11.8, 17.1, 20.2, 28.4, 87.9, 113.1, 113.2, 124.2, 126.4, 136.4, 137.3, 139.1, 146.1, 148.1, 155.3, 202.0; HRMS (ESI) calcd for $C_{29}H_{28}N_2O_3Se$ + H 533.1343, found 533.1342.

3-Bromo-8,13,14,19-tetraethyl-3,4-dihydro-3-hydroxy-3,9,18-trimethyl-4-oxo-2-oxybenziporphyrin (26). Bromine in acetic acid (36%; 106 μL; 1 equiv) was added to a stirred solution of **23** (10.0 mg, 0.019 mmol) in acetic acid (10 mL). The reaction mixture was stirred for 5 min and diluted with chloroform. The solution was washed with water, followed by saturated sodium bicarbonate solution, back-extracting with chloroform. The combined organic layers were evaporated down to dryness under reduced pressure, and the resulting brown residue was chromatographed on flash silica eluting with 50% dichloromethane−chloroform. The product fraction was collected and recrystallized from chloroform−hexanes to yield the bromo compound (5.1 mg, 0.0087 mmol, 45%) as brown crystals: mp >300 °C; UV−vis (1% Et_3N−$CHCl_3$) λ_{max} ($\log_{10}\varepsilon$) 400 (5.10), 513 (4.00), 546 (4.00), 596 (3.62), 657 nm (2.89); UV−vis (1% TFA−$CHCl_3$): λ_{max} ($\log_{10}\varepsilon$) 411 (5.13), 426 (5.14), 534 (3.95), 570 (3.87), 586 nm (3.97); ^{1}H NMR (500 MHz, $CDCl_3$) δ −7.45 (1H, s), 1.83 (12H, t, J = 7.7 Hz), 2.78 (3H, s), 3.59 (6H, s), 3.91 (4H, q, J = 7.7 Hz), 4.09−4.17 (4H, m), 9.72 (2H, s), 10.58 (2H, s); ^{1}H NMR (500 MHz, TFA−$CDCl_3$) δ −6.55 (1H, s), −5.63 (1H, br s), −2.68 (2H, br s), 1.61 (6H, t, J = 7.7 Hz), 1.88 (6H, t,

J = 7.7 Hz), 2.75 (3H, s), 3.55 (6H, s), 4.05−4.15 (8H, m), 10.13 (2H, s), 10.90 (2H, s); ^{13}C NMR ($CDCl_3$) δ 11.3, 17.5, 18.5, 19.9, 20.1, 21.0, 59.9, 95.0, 104.5, 119.0, 120.0, 130.4, 131.6, 138.9, 143.8, 145.2, 154.7, 194.5; FD MS m/z (rel int) 585 (M^+, 100), 586 (44), 587 (99), 589 (41). Anal. Calcd for $C_{33}H_{36}BrN_3O_2$: C, 67.57; H, 6.19; N, 7.16. Found: C, 67.42; H, 6.17; N, 7.11.

8,13,14,19-Tetraethyl-3,4-dihydro-3-hydroxy-3,9,18-trimethyl-4-oxo-2-oxybenziporphyrinatosilver(III) (30). Silver acetate (10.0 mg, 0.060 mmol) was added to a stirred solution of **24** (10.0 mg, 0.019 mmol) in dichloromethane (10 mL) and methanol (2.5 mL) and the mixture stirred overnight in a 25 mL round-bottom flask fitted with a drying tube and protected from light with aluminum foil. The resulting mixture was washed with water, back-extracting with chloroform, and the solvent was removed under reduced pressure. The dark red residue was chromatographed on flash silica eluting with 50% dichloromethane−chloroform to give the product as a dark orange fraction. Recrystallization from chloroform−hexanes yielded the silver(III) complex (10.5 mg, 0.0167 mmol, 87%) as red crystals: mp >300 °C; UV−vis ($CHCl_3$) λ_{max} ($\log_{10}\varepsilon$) 388 (4.49), 422 (4.83), 508 (3.91), 542 (4.23), 580 nm (4.02); ^{1}H NMR (500 MHz, $CDCl_3$) δ 1.66 (3H, s), 1.67−1.72 (12H, m), 3.32 (6H, s), 3.71−3.89 (8H, m), 4.80 (1H, s), 9.19 (2H, s), 9.91 (2H, s); ^{13}C NMR ($CDCl_3$) δ 12.1, 17.6, 18.3, 19.7, 20.1, 29.4, 82.7, 97.1, 111.8, 131.0, 134.90, 134.92, 136.5, 137.3, 141.1, 141.2, 199.7; HRMS (FAB) calcd for $C_{33}H_{34}AgN_3O_3$ + H 628.1729, found 628.1728. Anal. Calcd for $C_{33}H_{34}AgN_3O_3 \cdot {}^1/_8CHCl_3$: C, 61.83; H, 5.34; N, 6.53. Found: C, 61.89; H, 5.30; N, 6.53.

8,13,14,19-Tetraethyl-3,4-dihydro-3-hydroxy-3,9,18,23-tetramethyl-4-oxo-2-oxybenziporphyrin (31a). Potassium carbonate (300 mg) and 10 drops of iodomethane were added to a solution of **24** (29.7 mg, 0.057 mmol) in acetone (30 mL), and the resulting mixture was stirred under reflux overnight. The mixture was diluted in chloroform and washed with water, back-extracting with chloroform, and the solvent removed under reduced pressure. The red residue was chromatographed on flash silica eluting with 50% dichloromethane−chloroform, and the product collected as a yellowish purple fraction. The solvent was removed under reduced pressure to give the *N*-methyl derivative (21.0 mg, 0.039 mmol, 70%) as a purple solid. The NMR spectra indicate that the product consists of a mixture of two diastereomers in a ratio of approximately 2:1: UV−vis (Et_3N−$CHCl_3$) λ_{max} (rel int) 416 (1.00), 523 (0.12), 564 (0.11), 591 (0.10), 644 nm (0.05); UV−vis (TFA−$CHCl_3$) λ_{max} (rel int) 405 (1.00), 418 (0.91), 525 (0.07), 563 (0.05), 578 nm (0.07); ^{1}H NMR (major diastereomer, 500 MHz, $CDCl_3$) δ −5.73 (1H, s), −4.54 (3H, s), −2.0 (1H, v br), 1.34 (3H, t, J = 7.7 Hz), 1.55 (3H, s), 1.77 (3H, t, J = 7.7 Hz), 1.86−1.91 (6H, m), 3.18 (3H, s), 3.44 (3H, s), 3.70 (2H, q, J = 7.7 Hz), 3.88−4.07 (6H, m), 9.62 (1H, s), 9.71 (1H, s), 10.52 (1H, s), 10.54 (1H, s); ^{1}H NMR (minor diastereomer, 500 MHz, $CDCl_3$) δ −5.84 (1H, s), −4.71 (3H, s), −2.0 (1H, v br), 1.40 (3H, t, J = 7.7 Hz), 1.81 (3H, t, J = 7.7 Hz), 1.88−1.92 (6H, m), 2.31 (3H, s), 3.24 (3H, s), 3.48 (3H, s), 3.76 (2H, q, J = 7.7 Hz), 3.88−4.07 (6H, m), 9.69 (1H, s), 9.74 (1H, s), 10.18 (1H, s), 10.47 (1H, s); HRMS (FAB) calcd for $C_{34}H_{39}N_3O_3$ + H 538.3070, found 538.3069.

8,13,14,19,23-Pentaethyl-3,4-dihydro-3-hydroxy-3,9,18-trimethyl-4-oxo-2-oxybenziporphyrin (31b). Potassium carbonate (300 mg) and 10 drops of iodoethane were added to a solution of **24** (20.1 mg, 0.0384 mmol) in butanone (30 mL), and the resulting mixture was stirred under reflux overnight. The mixture was diluted in chloroform and washed with water, back-extracting with chloroform, and the solvent removed under reduced pressure. The red residue was purified by flash chromatography on silica eluting with 50% dichloromethane−chloroform, and the product collected as a yellowish-purple fraction. The solvent was removed under reduced pressure to give the *N*-ethyl derivative (14.2 mg, 0.0258 mmol, 67%) as a purple solid. The NMR spectra indicate that the product consists of a mixture of two diastereomers in a ratio of approximately 2:1: UV−vis (1% Et_3N−$CHCl_3$) λ_{max} (rel int) 413 (1.00), 528 (0.11), 564 (0.09), 592 (0.09), 647 nm (0.05); UV−vis (1% TFA−$CHCl_3$) λ_{max} (rel int) 406 (1.00), 419 (0.91), 525 (0.08), 580 nm (0.08); ^{1}H NMR (major diastereomer, $CDCl_3$) δ −5.76 (1H, s), −5.31 (1H, m), −4.90 (1H, m), −3.18 (1H, br s), −2.07 (3H, t, J = 7.0 Hz), 1.29 (3H, t,, J = 7.6 Hz), 1.63 (3H, s), 1.78 (3H, t, J = 7.7 Hz), 1.86−1.92 (6H, m), 3.19 (3H, s), 3.45 (3H, s), 3.69−3.84 (2H, m), 3.89−4.09 (6H, m), 9.70 (1H, s), 9.71 (1H, s), 10.53 (1H, s), 10.61 (1H, s); ^{1}H NMR (minor diastereomer, $CDCl_3$) δ −5.92 (1H, s), −5.41 (1H, m), −5.11 (1H, m), −3.18 (1H, br s), −2.20 (3H, t, J = 7.8 Hz), 1.35 (3H, t, J = 7.7 Hz), 1.78 (3H, s), 1.81 (3H, t,, J = 7.6 Hz), 1.86−1.92 (12H, m), 2.23 (3H, s), 3.24 (3H, s), 3.48 (3H, s), 3.69−3.84 (2H, m), 3.89−4.09 (6H, m), 9.71 (1H, s), 9.79 (1H, s), 10.29 (1H, s), 10.44 (1H, s); HRMS (ESI) calcd for $C_{35}H_{41}N_3O_3$ + H 552.3226, found 552.3228.

Crystallographic Experimental Details of 28b·MeOH. X-ray quality crystals for the methanol solvate of **28b** were suspended in mineral oil at ambient temperature, and a suitable crystal was selected. A mineral oil coated black block thereby obtained of approximate dimensions 0.70 × 0.51 × 0.43 mm^3 was mounted on a 50 μm polyimide micromount and transferred to a CCD-equipped X-ray diffractometer. The X-ray diffraction data were collected at −173 °C using Mo Kα (λ = 0.71073 Å) radiation. Data collection and cell refinement were performed using SMART and SAINT+, respectively.[48] The unit cell parameters were obtained from a least-squares refinement of 6734 centered reflections. Compound **28b·MeOH** was found to crystallize in the monoclinic crystal system with the following unit cell parameters: a = 9.3698(9) Å, b = 12.850(1) Å, c = 21.309(2) Å, β = 94.857(2)°, Z = 4. The systematic absences indicated the space group to be $P2_1/n$ (no. 14).[49] A total of 25832 reflections were collected, of which 6349 were unique, and 5751 were observed $F_o^2 > 2\,\sigma(F_o^2)$. Limiting indices were as follows: $-12 \le h \le 12$, $-17 \le k \le 17$, $-28 \le l \le 28$. Data reduction were accomplished using SAINT.[47] The data were corrected for absorption using the SADABS procedure.[49]

Solution and data analysis were performed using the WinGX software package.[50] The structure of **28b·MeOH** was solved by charge-flipping methods using the program SUPERFLIP,[51] and the refinement was completed using the program SHELX-97.[52] All non-H atoms were refined anisotropically. With the exception of the NH H atom, all H atoms were included in the refinement in the riding-model approximation (C−H = 0.95, 0.98, and 0.99 Å for Ar−H, CH_3, and CH_2; U_{iso}(H) = 1.2U_{eq}(C) except for methyl groups, where U_{iso}(H) = 1.5eq(C); O−H = 0.84 Å; U_{iso}(H) = 1.5U_{eq}(O)) with CH_3 and OH torsions taken from electron density. The NH H atom was freely refined because it was clearly visible in the difference Fourier map and placement in the idealized riding model position would force it into space blocked by the Se atom of the macrocycle. Full-matrix least-squares refinement on F^2 led to convergence, $(\Delta/\sigma)_{max}$ = 0.000, $(\Delta/\sigma)_{mean}$ = 0.0000, with R_1 = 0.0275 and wR_2 = 0.0757 for 6349 data with $F_o^2 > 2\sigma(F_o^2)$ using 0 restraints and 346 parameters. A final difference Fourier synthesis showed features in the range of $\Delta\rho_{max}$ = 0.65 e$^-$/Å^3 to $\Delta\rho_{min}$ = −0.485 e$^-$/Å^3, which were deemed of no chemical significance. Molecular diagrams were generated using ORTEP-3.[53] CCDC 826847 contains the supplementary crystallographic data for this paper. These data can be obtained free of charge from The Cambridge Crystallographic Data Centre via www.ccdc.cam.ac.uk/data_request/cif.

■ ASSOCIATED CONTENT

Supporting Information. Crystallographic data for **28b** (CIF) and MS, UV−vis, IR, ^{1}H NMR, COSY, HSQC, DEPT-135, and ^{13}C NMR spectra for selected compounds. This material is available free of charge via the Internet at http://pubs.acs.org.

AUTHOR INFORMATION

Corresponding Author

*E-mail: tdlash@ilstu.edu.

Notes

†Conjugated Macrocycles Related to the Porphyrins. 58. For part 57, see ref 44d.

ACKNOWLEDGMENT

This work was supported by the National Science Foundation under Grant Nos. CHE-0616555 and CHE-0911699 and the Petroleum Research Fund, administered by the American Chemical Society. Funding for a 500 MHz NMR spectrometer was provided by the National Science Foundation under Grant No. CHE-0722385. K.M. and L.X. thank Abbott Laboratories for providing summer graduate fellowships. We also thank Youngstown State University Structure & Chemical Instrumentation Facility's Matthias Zeller for X-ray data collection. The diffractometer was funded by NSF Grant No. 0087210, Ohio Board of Regents Grant No. CAP-491, and YSU.

REFERENCES

(1) Berlin, K.; Breitmaier, E. *Angew. Chem., Int. Ed. Engl.* **1994**, *33*, 1246–1247.

(2) Lash, T. D. *Angew. Chem., Int. Ed. Engl.* **1995**, *34*, 2533–2535.

(3) (a) Lash, T .D.; Chaney, S. T.; Richter, D. T. *J. Org. Chem.* **1998**, *63*, 9076–9088. (b) Liu, D.; Lash, T. D. *Chem. Commun.* **2002**, 2426–2427. (c) Jiao, W.; Lash, T. D. *J. Org. Chem.* **2003**, *68*, 3896–3901. (d) Liu, D.; Ferrence, G. M.; Lash, T. D. *J. Org. Chem.* **2004**, *69*, 6079–6093.

(4) Stepien, M.; Latos-Grazynski, L. *Acc. Chem. Res.* **2005**, *38*, 88–98.

(5) Stepien, M.; Latos-Grazynski, L. *Chem.—Eur. J.* **2001**, *7*, 5113–5117.

(6) Lash, T. D.; Yant, V. R. *Tetrahedron* **2009**, *65*, 9527–9535.

(7) (a) Stepien, M.; Latos-Grazynski, L.; Szterenberg, L.; Panek, J.; Latajka, Z. *J. Am. Chem. Soc.* **2004**, *126*, 4566–4580. (b) Stepien, M.; Latos-Grazynski, L. *Org. Lett.* **2003**, *5*, 3379–3381. (c) Hung, C.-H.; Chang, F.-C.; Lin, C.-Y.; Rachlewicz, K.; Stepien, M.; Latos-Grazynski, L.; Lee, G.-H.; Peng, S.-M. *Inorg. Chem.* **2004**, *43*, 4118–4120. (d) Stepien, M.; Latos-Grazynski, L.; Szterenberg, L. *Inorg. Chem.* **2004**, *43*, 6654–6662.

(8) (a) Stepien, M.; Latos-Grazynski, L. *J. Am. Chem. Soc.* **2002**, *124*, 3838–3839. (b) Hung, C.-H.; Lin, C.-Y.; Lin, P.-Y.; Chen, Y.-J. *Tetrahedron Lett.* **2004**, *45*, 129–132.

(9) (a) Chang, G.-F.; Kumar, A.; Ching, W.-M.; Chu, H.-W.; Hung, C.-H. *Chem. Asian J.* **2009**, *4*, 164–173. (b) Huang, C.; Li, Y.; Yang, J.; Cheng, N.; Liu, H.; Li, Y. *Chem. Commun.* **2010**, *46*, 3161–3163.

(10) Richter, D. T.; Lash, T. D. *Tetrahedron* **2001**, *57*, 3659–3673.

(11) Szymanski, J. T.; Lash, T. D. *Tetrahedron Lett.* **2003**, *44*, 8613–8616.

(12) Lash, T. D.; Szymanski, J. T.; Ferrence, G. M. *J. Org. Chem.* **2007**, *72*, 6481–6492.

(13) Lash, T. D.; Young, A. M.; Rasmussen, J. M.; Ferrence, G. M. *J. Org. Chem.* **2011**, *76*, 5636–5651.

(14) Venkatraman, S.; Anand, V. G.; Pushpan, S. K.; Sankar, J.; Chandrashekar, T. K. *Chem. Commun.* **2002**, 462–463.

(15) El-Beck, J. A.; Lash, T. D. *Org. Lett.* **2006**, *8*, 5263–5266.

(16) Lash, T. D. In *The Porphyrin Handbook*; Kadish, K. M., Smith, K. M., Guilard, R., Eds.; Academic Press: San Diego, 2000; Vol. 2, pp 125−199.

(17) (a) Lash, T. D. *Synlett* **2000**, 279–295. (b) Lash, T. D. *Eur. J. Org. Chem.* **2007**, 5461–5481.

(18) Graham, S. R.; Colby, D. A.; Lash, T. D. *Angew. Chem., Int. Ed.* **2002**, *41*, 1371–1374.

(19) Lash, T. D.; Colby, D. A.; Graham, S. R.; Chaney, S. T. *J. Org. Chem.* **2004**, *69*, 8851–8864.

(20) Lash, T. D.; El-Beck, J. A.; Ferrence, G. M. *J. Org. Chem.* **2007**, *72*, 8402–8415.

(21) For other syntheses of azuliporphyrins, see: (a) Lash, T. D.; Chaney, S. T. *Angew. Chem., Int. Ed. Engl.* **1997**, *36*, 839–840. (b) Lash, T. D. *Chem. Commun.* **1998**, 1683–1684. (c) Venkatraman, S.; Anand, V. G.; PrabhuRaja, V.; Rath, H.; Sankar, J.; Chandrashekar, T. K.; Teng, W.; Senge, K. R. *Chem. Commun.* **2002**, 1660–1661. (d) Colby, D. A.; Ferrence, G. M.; Lash, T. D. *Angew. Chem., Int. Ed.* **2004**, *43*, 1346–1349. (e) Okujima, T.; Komobuchi, N.; Shimizu, Y.; Uno, H.; Ono, N. *Tetrahedron Lett.* **2004**, *45*, 5461–5464. (f) Lash, T. D.; Colby, D. A.; Idate, A. S.; Davis, R. N. *J. Am. Chem. Soc.* **2007**, *129*, 13801–13802. (g) Zhang, Z.; Ferrence, G. M.; Lash, T. D. *Org. Lett.* **2009**, *11*, 101–104.

(22) (a) Colby, D. A.; Lash, T. D. *J. Org. Chem.* **2002**, *67*, 1031–1033. (b) Lash, T. D.; El-Beck, J. A.; Colby, D. A. *J. Org. Chem.* **2009**, *74*, 8830–8833.

(23) (a) Colby, D. A.; Lash, T. D. *Chem.—Eur. J.* **2002**, *8*, 5397–5402. (b) Lash, T. D.; Colby, D. A.; Ferrence, G. M. *Eur. J. Org. Chem.* **2003**, 4533–4548. (c) El-Beck, J. A.; Lash, T. D. *Eur. J. Org. Chem.* **2007**, 3981–3190.

(24) For other applications of this concept, see: (a) Sprutta, N.; Swiderska, M.; Latos-Grazynski, L. *J. Am. Chem. Soc.* **2005**, *127*, 13108–13109. (b) Berlicka, A.; Sprutta, N.; Latos-Grazynski, L. *Chem Commun.* **2006**, 3346–3348. (c) Sprutta, N.; Siczek, M.; Latos-Grazynski, L.; Pawlicki, M.; Szterenberg, L.; Lis, T. *J. Org. Chem.* **2007**, *72*, 9501–9509. (d) Shoji, T.; Higashi, J.; Ito, S.; Toyota, K.; Iwamoto, T.; Morita, N. *Eur. J. Org. Chem.* **2009**, 5948–5952. (e) Sprutta, N.; Mackowiak, S.; Kocik, M.; Szterenberg, L.; Lis, T.; Latos-Grazynski, L. *Angew. Chem., Int. Ed.* **2009**, *48*, 3337–3341.

(25) Lash, T. D. *Chem.—Eur. J.* **1996**, *2*, 1197–1200.

(26) (a) Lin, Y.; Lash, T. D. *Tetrahedron Lett.* **1995**, *36*, 9441–9444. (b) Boudif, A.; Momenteau, M. *J. Chem. Soc., Perkin Trans. 1* **1996**, 1235–1241. (c) Sessler, J. L.; Genge, J. W.; Urbach, A.; Sanson, P. *Synlett* **1996**, 187–188. (d) Lash, T. D. *J. Porphyrins Phthalocyanines* **1997**, *1*, 29–44. (e) Lash, T. D.; Chandrasekar, P.; Osuma, A. T.; Chaney, S. T.; Spence, J. D. *J. Org. Chem.* **1998**, *63*, 8455–8469.

(27) Preliminary communication: Miyake, K.; Lash, T. D. *Chem. Commun.* **2004**, 178–179.

(28) Jackson, A. H.; Pandey, R. K.; Rao, K. N. R.; Roberts, E. *Tetrahedron Lett.* **1985**, *26*, 793–796.

(29) (a) Clezy, P. S.; Liepa, A. J. *Aust. J. Chem.* **1970**, *23*, 2443–2459. (b) Lash, T. D. *Tetrahedron* **1998**, *54*, 359–374.

(30) Bromine readily oxidizes dipyrrylmethanes to conjugated dipyrromethenes. Presumably, bromine vapor also oxidizes the benzitripyrranes to conjugated species.

(31) Tardieux, C.; Bolze, F.; Gros, C. P.; Guilard, R. *Synthesis* **1998**, 267–268.

(32) (a) Lash, T. D.; Richter, D. T.; Shiner, C. M. *J. Org. Chem.* **1999**, *64*, 7973–7982. (b) Richter, D. T.; Lash, T. D. *Tetrahedron Lett.* **1999**, *40*, 6735–6738. (c) Richter, D. T.; Lash, T. D. *J. Org. Chem.* **2004**, *69*, 8842–8850.

(33) Medforth, C. J. In *The Porphyrin Handbook*; Kadish, K. M., Smith, K. M., Guilard, R., Eds.; Academic Press: San Diego, 2000; Vol. 5, pp 1−80.

(34) Latos-Grazynski, L.; Pacholska, E.; Chmielewski, P. J.; Olmstead, M. M.; Balch, A. L. *Inorg. Chem.* **1996**, *35*, 566–573.

(35) Pushpan, S. K.; Srinivasan, A.; Anand, V. R. G.; Chandrashekar, T. K.; Subramanian, A. R.; Roy, R.; Sugiura, K.; Sakata, Y. *J. Org. Chem.* **2001**, *66*, 153–161.

(36) Mysliborski, R.; Latos-Grazynski *Eur. J. Org. Chem.* **2005**, 5039–5048.

(37) Allen, F. H. *Acta Crystallogr.* **2002**, *B58*, 380–388.

(38) Furuta, H.; Ogawa, T.; Uwatoko, Y.; Araki, K. *Inorg. Chem.* **1999**, *38*, 2676–2682.

(39) Lash, T. D.; Rasmussen, J. M.; Bergman, K. M.; Colby, D. A. *Org. Lett.* **2004**, *6*, 549–552.
(40) (a) Muckey, M. A.; Szczepura, L. F.; Ferrence, G. M.; Lash, T. D. *Inorg. Chem.* **2002**, *41*, 4840–4842. (b) Lash, T. D.; Colby, D. A.; Szczepura, L. F. *Inorg. Chem.* **2004**, *43*, 5258–5267.
(41) Bergman, K. M.; Ferrence, G. M.; Lash, T. D. *J. Org. Chem.* **2004**, *69*, 7888–7897.
(42) N-Confused porphyrins can also act as dianionic ligands and may take on more complex coordination motifs. See: (a) Latos-Grazynski, L. In *The Porphyrin Handbook*; Kadish, K. M., Smith, K. M., Guilard, R., Eds.; Academic Press: San Diego, 2000; Vol. 2, pp 361−416. (b) Srinivasan, A.; Furuta, H. *Acc. Chem. Res.* **2005**, *38*, 10–20. (c) Harvey, J. D.; Ziegler, C. J. *Coord. Chem. Rev.* **2003**, *247*, 1–19.
(43) Benziporphyrins commonly act as dianionic ligands.[7] In addition, oxybenziporphyrin can also act as a dianionic ligand as well. Stepien, M.; Latos-Grazynski, L.; Lash, T. D.; Szterenberg, L. *Inorg. Chem.* **2001**, *40*, 6892–6900.
(44) For other examples of organometallic derivatives of carbaporphyrinoid systems, see: (a) Graham, S. R.; Ferrence, G. M.; Lash, T. D. *Chem. Commun.* **2002**, 894–895. (b) Lash, T. D.; Colby, D. A.; Graham, S. R.; Ferrence, G. M.; Szczepura, L. F. *Inorg. Chem.* **2003**, *42*, 7326–7338. (c) Lash, T. D.; Young, A. M.; Von Ruden, A. L.; Ferrence, G. M. *Chem. Commun.* **2008**, 6309–6311.(d) Young, A. M.; Von Ruden, A. L.; Lash, T. D. *Org. Biomol. Chem.* **2011**, DOI:10.1039/C1OB05603D. (e) Lash, T. D. *Macroheterocycles* **2008**, *1*, 9–20.
(45) (a) Daniell, H. W.; Brückner, C. *Angew. Chem., Int. Ed.* **2004**, *43*, 1688–1691. (b) Chmielewski, P. J.; Szterenberg, L.; Siczek, M. *Chem.—Eur. J.* **2011**, *17*, 1009–1020.
(46) Tripyrrane analogues **20a** and **20b** were also used to prepare dicarbaporphyrinoid systems: See, Xu, L.; Lash, T. D. *Tetrahedron Lett.* **2006**, *47*, 8863–8866.
(47) Johnson, A. W.; Kay, I. T.; Markham, E.; Price, R.; Shaw, K. B. *J. Chem. Soc.* **1959**, 3416–3424.
(48) APEX2 v2008.2−4, Bruker AXS, Inc., Madison, WI, 2008.
(49) McArdle, P. *J. Appl. Crystallogr.* **1996**, *29*, 306.
(50) Farrugia, L. J. *J. Appl. Crystallogr.* **1999**, *32*, 837–838.
(51) Palatinus, L.; Chapuis, G. *J. Appl. Crystallogr.* **2007**, *40*, 786–790.
(52) Sheldrick, G. M. *Acta Crystallogr.* **2008**, *A64*, 112–122.
(53) Farrugia, L. J. *J. Appl. Crystallogr.* **1997**, *30*, 565.